SIEMENS

Imaging Life

The Magazine for Molecular Imaging Innovation

Clinical Case Supplement | xSPECT Edition

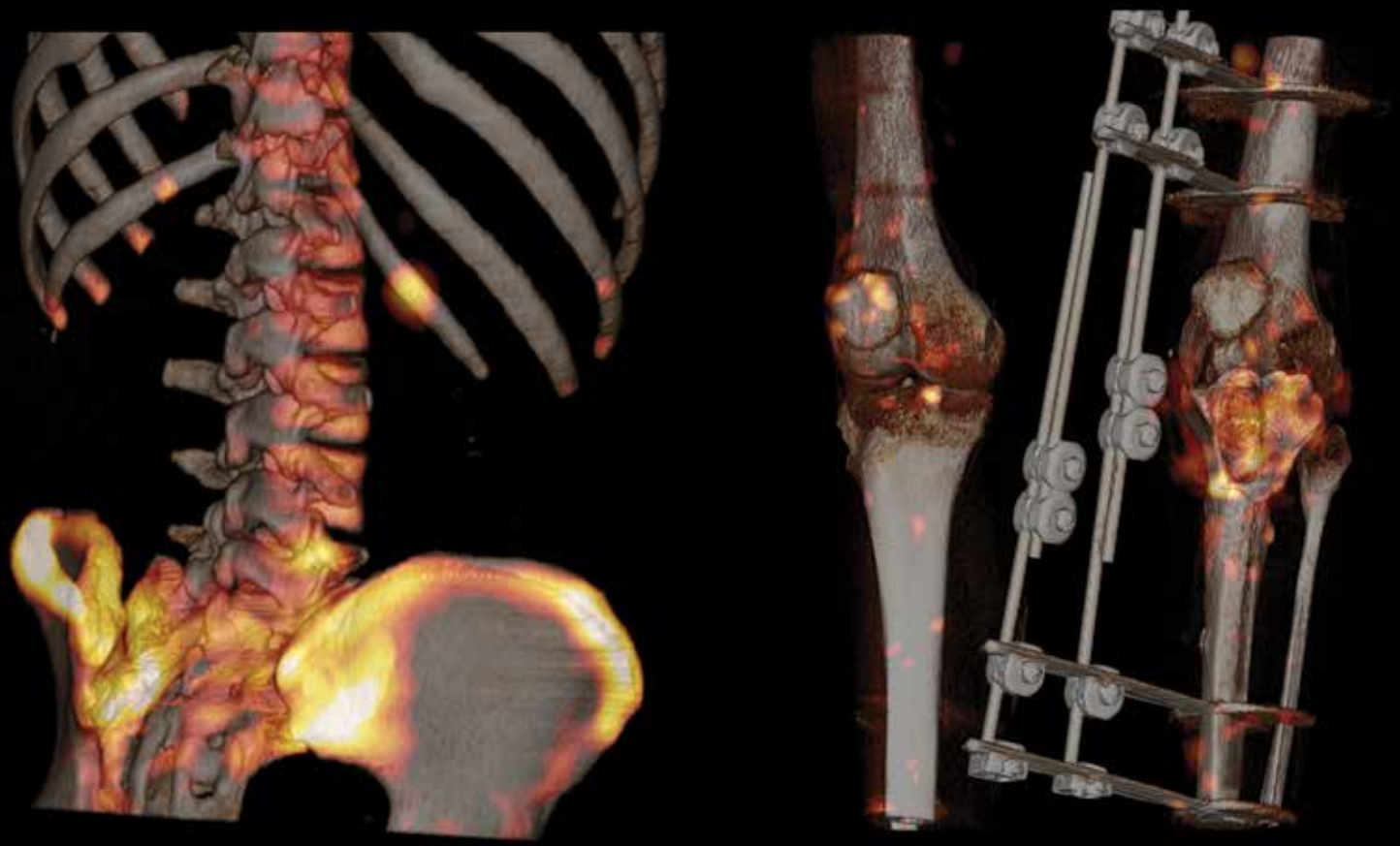

Table of Contents

Clinical Results

Case 1

Delineation of Aseptic Loosening of Hip Prosthesis with ^{99m}Tc MDP Bone SPECT/CT and xSPECT Bone Reconstruction

By Christian Waldherr, MD, and Martin Sonnenschein, MD

Data courtesy of the Department of Radiology & Nuclear Medicine, Klinik Engeried, Bern, Switzerland

History

A 67-year-old woman with a history of total hip arthroplasty, performed 3 years back, presented with persistent pain in the affected left hip. The patient was referred for a ^{99m}Tc MDP bone SPECT/CT. The study was performed 3 hours following an IV injection of 600 MBq (16.22 mCi) of ^{99m}Tc MDP. A non-contrast diagnostic CT was performed followed by SPECT acquisition (32 stops per detector, 20 sec/stop). Images were reconstructed using xSPECT Bone*, a unique reconstruction algorithm that leverages CT-based tissue class information.

Diagnosis

The ^{99m}Tc MDP bone SPECT maximum intensity projection (MIP) image (*Figure 1*) showed focal area of increased uptake in the left acetabulum and slightly increased uptake in the upper part of femoral shaft (*Figure 2*). Fused xSPECT images showed areas of osteolysis and lucency in the acetabulum bordering the acetabular cup (*Figure 1, thin red arrows*). Peri-implant radiolucency in those areas that interface between the prosthesis and the surrounding bone (Gruen zones) are usually associated with prosthetic loosening, especially when

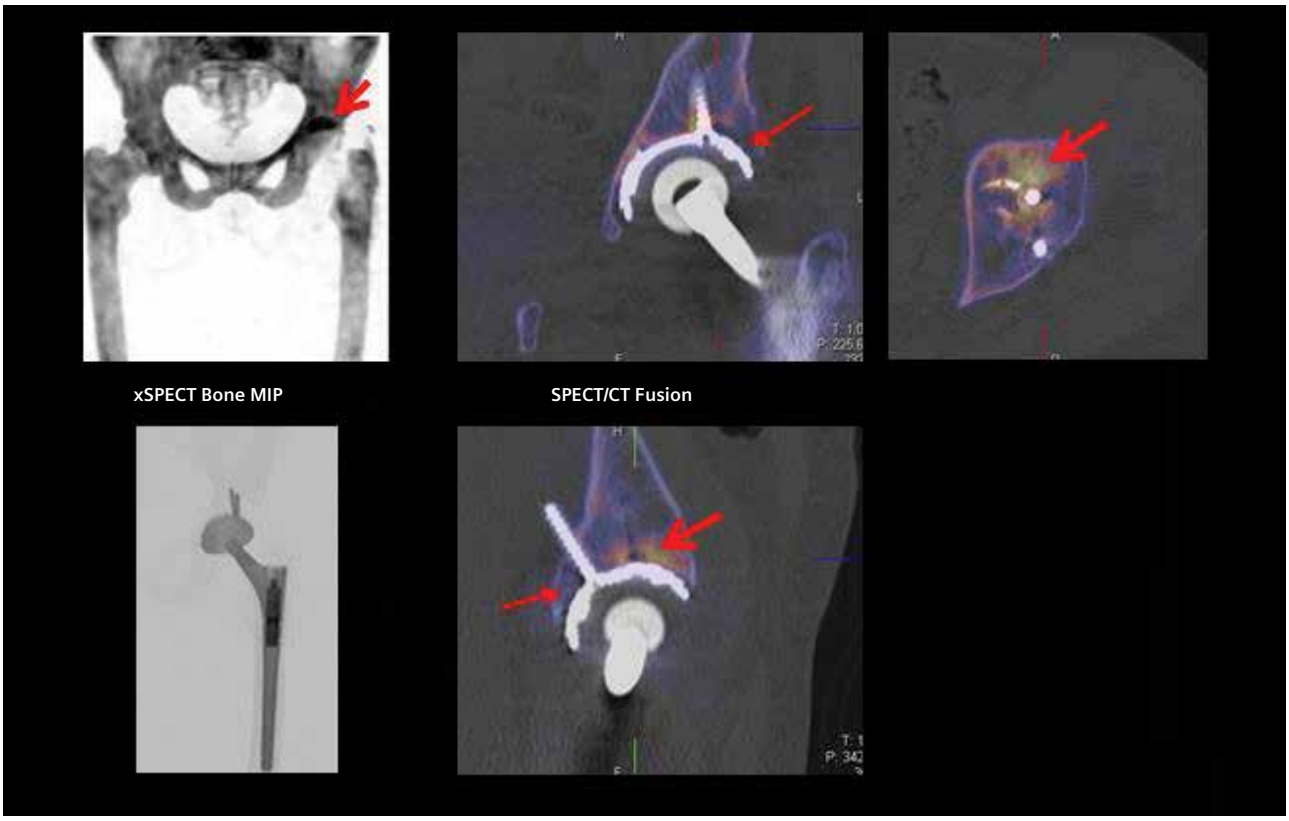

Figure 1: SPECT MIP image shows focal area of increased uptake in the left acetabulum (*bold red arrow*). Fused xSPECT images show zones of osteolysis and lucency bordering the acetabular cup (*thin red arrows*). Areas of osteolysis and increased uptake of tracer around the acetabular screw (*bold red arrow on fused images*) reflect loosening related to periprosthetic bone stress.

the periprosthetic osteolysis is >2 mm—as was the case with the acetabular lucency seen on the SPECT/CT.

Osteolysis and increased uptake of ^{99m}Tc MDP was visualized around the acetabular screw (*bold red arrow*); this reflected increased bone stress, secondary to screw loosening. Osteolysis around the fixation screw is often the earliest and, probably, the most specific sign of loosening.

Reconstructed images of the upper part of the femoral shaft and the associated part of the stem of the prosthesis showed zones of lucency between the edge of the prosthesis and the adjacent proximal femoral bone (*Figure 2, fused images, thin red arrows*).

Increase in peri-implant lucency in the femoral Gruen zones was associated with prosthetic loosening. The pattern of ^{99m}Tc MDP uptake adjacent to the acetabular screw, and at the edge of the stem of the femoral component of the prosthesis, revealed loosening. The patient was advised revision arthroplasty.

Comments

Pain is a common complication following orthopedic surgery. Pain could be secondary to a variety of causes that are often difficult to distinguish clinically and diagnostically.

Due to metal artifacts found in MRI, bone overlays in X-ray and proximity to the tracer filled bladder in SPECT, assessing loosening of the hip component can be very difficult.

The SPECT agent ^{99m}Tc MDP identified osseous pathologies and offered a severity grading in comparison to other regional uptakes, as well as in comparison with potential hyperemia/inflammation/synovitis shown in the blood pool phase.

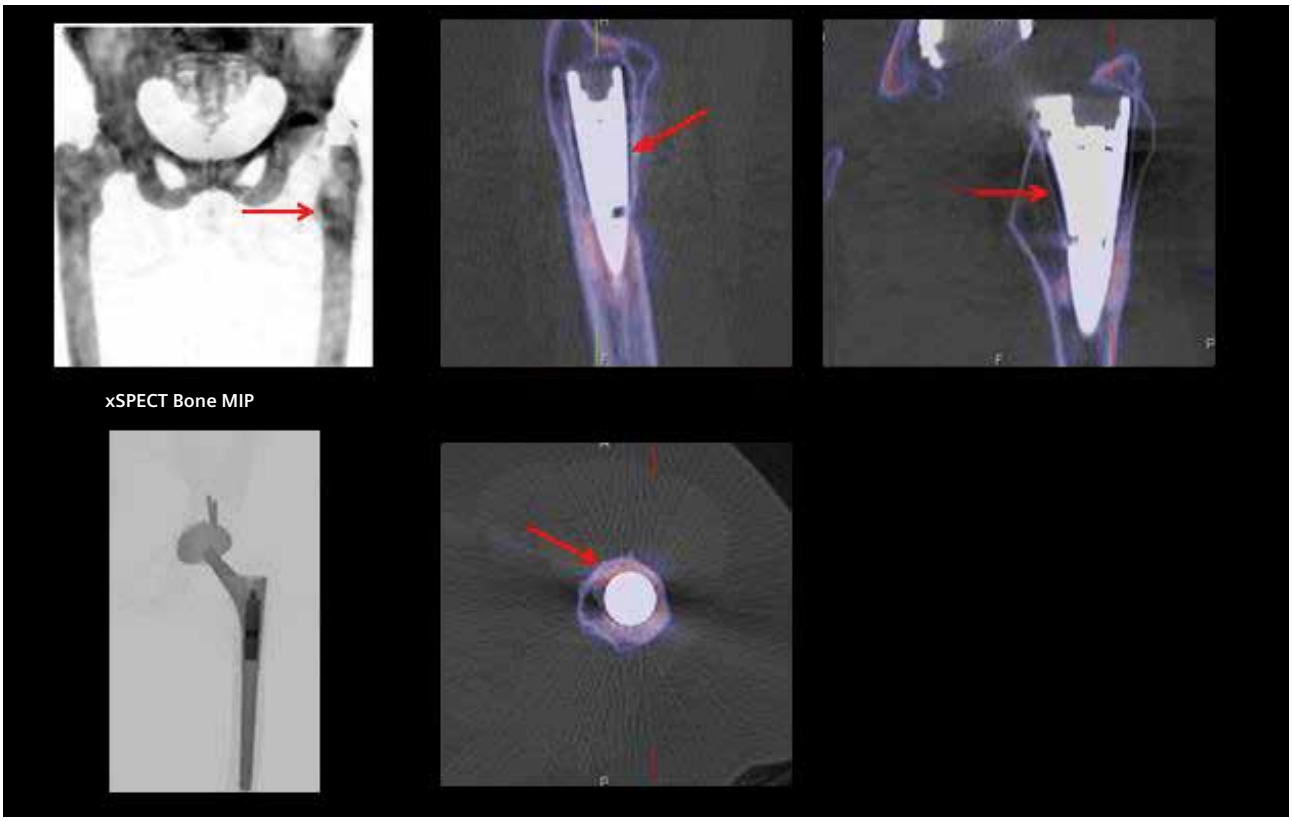

Figure 2: SPECT MIP image shows mild linear increase in uptake in the upper third of the femoral shaft and lesser trochanter. Fused xSPECT images show radiolucent zones between the margin of the prosthesis and adjacent bone (*thin red arrows*), with part of these zones showing mild increase in uptake, which suggests bone stress related to loosening.

xSPECT Bone can help improve definition and lesion contrast of small focal areas of increased uptake, which are often seen in early prosthetic loosening, as was the case in this example.

The diagnostic CT component of SPECT/CT allowed the evaluation and diagnosis of the osseous stress reactions and demonstrated non-hypermetabolic pathologies as foreign body granuloma, metallosis, foreign bodies, disc hernia or muscle degeneration (not visible in SPECT and in low-dose CT, and difficult to interpret by physicians not trained in musculoskeletal radiology).

Common causes are periprosthetic bone loss leading to joint instability, shear stress, head displacements and increased joint pressures. Debris from prosthetic joints produced by wear at the articulating surfaces may induce bone resorption (osteolysis) and formation of fibrous tissue. Typical findings of loosening of prosthetic hip joint include periprosthetic osteolysis; increased lucency in the Gruen zones, which are the interfaces between the prosthetic margin; and adjacent bone and scintigraphic evidence of shear stress reflected by hypermetabolism at focal areas like screws or edges of femoral prosthetic stem, or at the end of the femoral stem reflecting the instability and motion of the prosthetic joint.

Typically, an osseous stress reaction is limited or reduced in the area of osteolysis in the proximal femur where the prosthesis can already move. These lucencies extend along the proximal femoral stem of the prosthesis. And commonly, the osseous stress reaction is increased in the area of the still-fixed prosthesis around the mid or distal prosthesis.

A typical pattern of skeletal scintigraphy in aseptic loosening of hip prosthesis (Kobayashi classification: Type 2 minor uptake) is associated with minor uptake in the cup side, usually associated with the acetabular screw; and minor uptake in the stem, usually towards the end of the shaft of the femoral prosthesis. The two uptake patterns may coexist.[1] In the present case, the scintigraphic pattern, the CT findings of increased lucency (>2mm)

in the acetabular and the femoral Gruen zones[2] contribute to the SPECT/CT diagnosis of a loosening hip prosthesis. A combination of metabolic information of bone stress seen on SPECT and periprosthetic lucency defined on diagnostic CT enabled comprehensive evaluation of prosthetic loosening with SPECT/CT.

Conclusion

The combination of a 3-phase bone scan, whole-body scan and diagnostic SPECT/CT with xSPECT Bone led to a whole-body coverage and comprehensive evaluation of the target region, along with adjacent joints—all of which is key to evaluating pain syndromes and the post-operative orthopedic patient. ■

Examination Protocol

Scanner: Symbia Intevo™*

SPECT	
Injected Dose	600 MBq (16.22 mCi) ^{99m}Tc MDP
Scan Delay	3 hours
Acquisition	64 projections, 20 sec/stop

CT	Non-contrast diagnostic
Tube Voltage	110 kV
Tube Current	120 eff mAs
Slice Collimation	16 x 2.5 mm
Slice Thickness	3 mm

References:
[1] Kitajima et al. *Eur J Nucl Med Mol Imaging*. 2009; 36: 362-372.
[2] Keogh et al. *Am J Roentgenol*. 2003 Jan; 180(1): 115-120.

* Symbia Intevo and xSPECT Bone are not commercially available in all countries. Due to regulatory reasons their future availability cannot be guaranteed. Please contact your local Siemens organization for further details.

Case 2

Improved Delineation by xSPECT Bone of Loosening of Femoral Component of Hip Prosthesis

By Xuan Pham, MD, and François Raymond, MD

Data courtesy of CSSS de Gatineau, Hôpital de Hull, Hull, Canada

History

A 49-year-old man, who had a history of right total hip arthroplasty performed 3 years prior, presented with persistent pain in the affected right hip. Thus, the patient was referred to ^{99m}Tc MDP bone SPECT/CT. The study was performed 3 hours following an IV injection of 500 MBq (13.5 mCi) of ^{99m}Tc MDP on a Symbia Intevo™* 16 scanner. A non-contrast diagnostic CT (130 kV, 45 eff mAs, 2 mm slice thickness) was performed, followed by a SPECT acquisition (32 stops, 20 sec/stop). xSPECT Bone* reconstruction was performed using CT-based zone information.

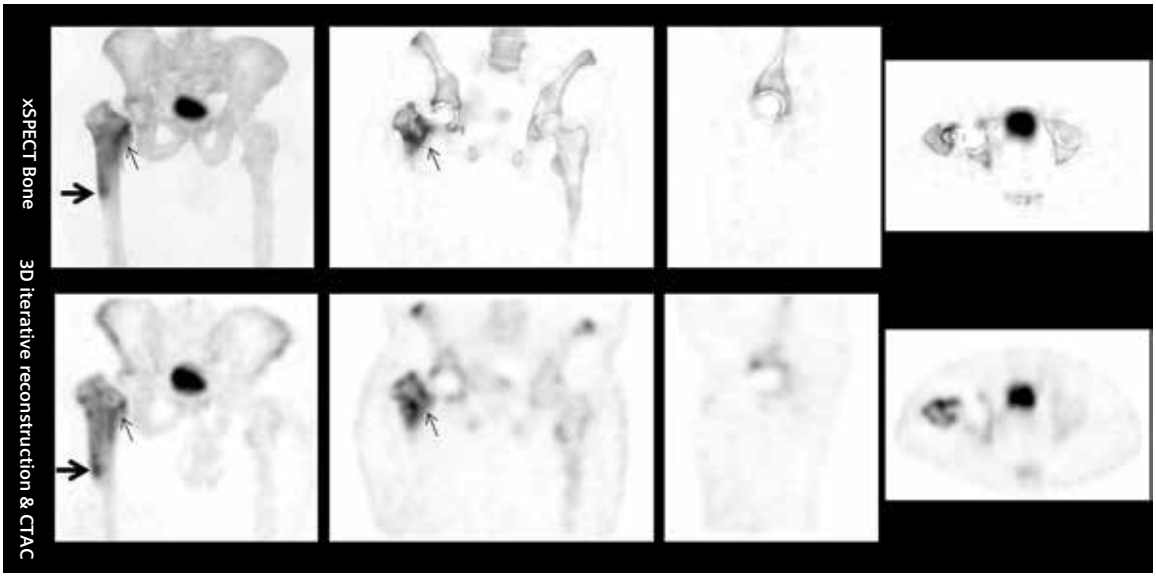

Figure 1: Comparison between maximum intensity projection (MIP) and multiplanar reformatting (MPR) images of 3D iterative reconstruction and xSPECT Bone shows focal area of increased uptake at the margins of the femoral component of the right hip prosthesis, with the highest uptake at the tip of the stem (*bold arrows*). There is also increased uptake in the region of the lesser trochanter (*thin arrows*). The femoral head and acetabulum show normal uptake. xSPECT Bone images show sharper definition of periprosthetic hypermetabolism as well as that of acetabular and pelvic cortical margins as compared to standard 3D iterative reconstruction images.

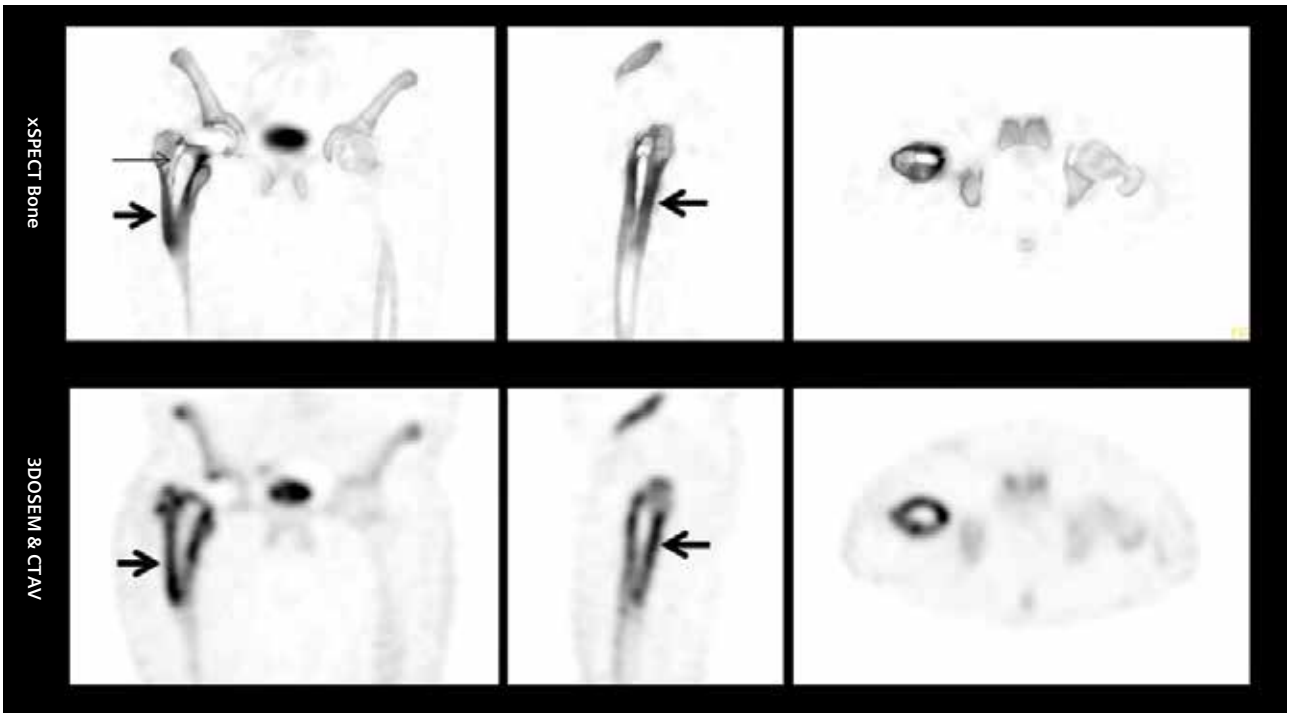

Figure 2: Comparison images show intense tracer uptake (*bold arrows*) around the stem of the femoral component of the total hip prosthesis. xSPECT Bone images also show thin translucent zones adjacent to the right lateral edge of the femoral component of the prosthesis (*thin arrow*) that reflects an enlarged Gruen zone. The uptake around the femoral component with highest uptake at the tip of the stem along with the peri-implant lucent zone suggests loosening of the femoral component.

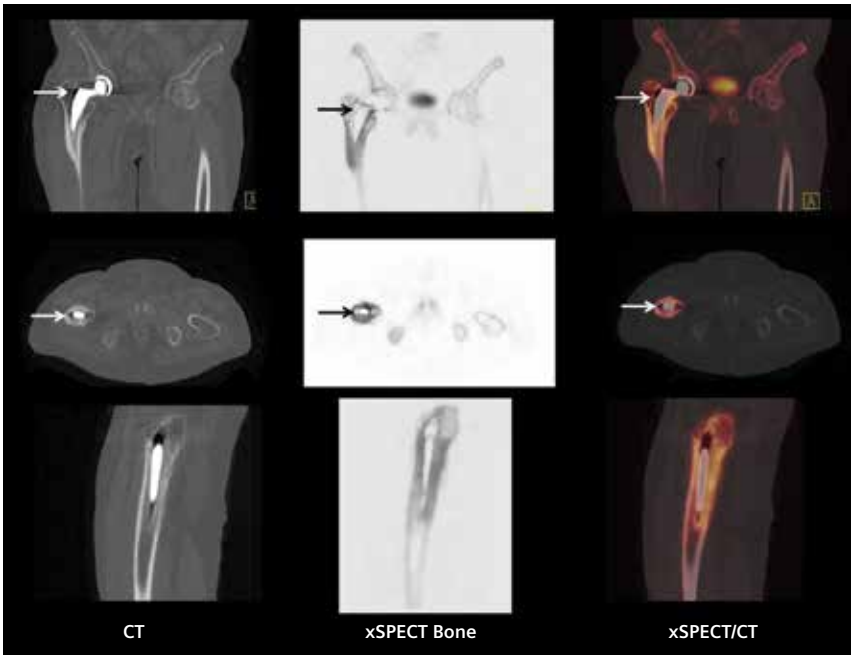

Figure 3: CT shows peri-prosthetic radiolucent zones, enlarged Gruen zones (*arrows*). Fused xSPECT and CT images show increased uptake in the cortical bone adjacent to the stem of the femoral component of the prosthesis. The uptake pattern suggests loosening of the femoral component.

Diagnosis
xSPECT Bone images (*Figures 1 & 2*) showed increased uptake around the stem of the femoral component of the hip prosthesis, with peri-implant translucent zones in the lateral aspect of the stem. CT showed peri-implant radiolucent zones (Gruen zones) especially in the shaft of the femoral component at the trochanteric level. Fused images showed increased uptake throughout the stem of the femoral component, with very high uptake at the tip of the stem and in the lesser trochanter, which may reflect shear stress due to loosening. However, infection of the prosthesis may also appear similar in bone SPECT.

The peri-implant zones of osteolysis and lucency and high uptake in the tip of the stem were in favor of loosening. Peri-implant radiolucency in areas that interface between the prosthesis and the surrounding bone (Gruen zones) is usually associated with prosthetic loosening, especially when the peri-prosthetic radiolucency is >2 mm, as in this example. Since the pattern of uptake involving the entire stem of the femoral part of the prosthesis may also be found in infection, the patient was referred for a ^{111}In-labelled WBC SPECT/CT study for infection imaging, even though the radiological impression from xSPECT Bone was more in favor of loosening.

Comments
Loosening of hip prosthesis is a common complication after total hip arthroplasty, and SPECT/CT is often helpful in differentiating between loosening and infection. ^{99m}Tc MDP bone SPECT/CT often demonstrates a typical pattern of focal increase in uptake around loosened screws or at the tip of the stem reflecting the

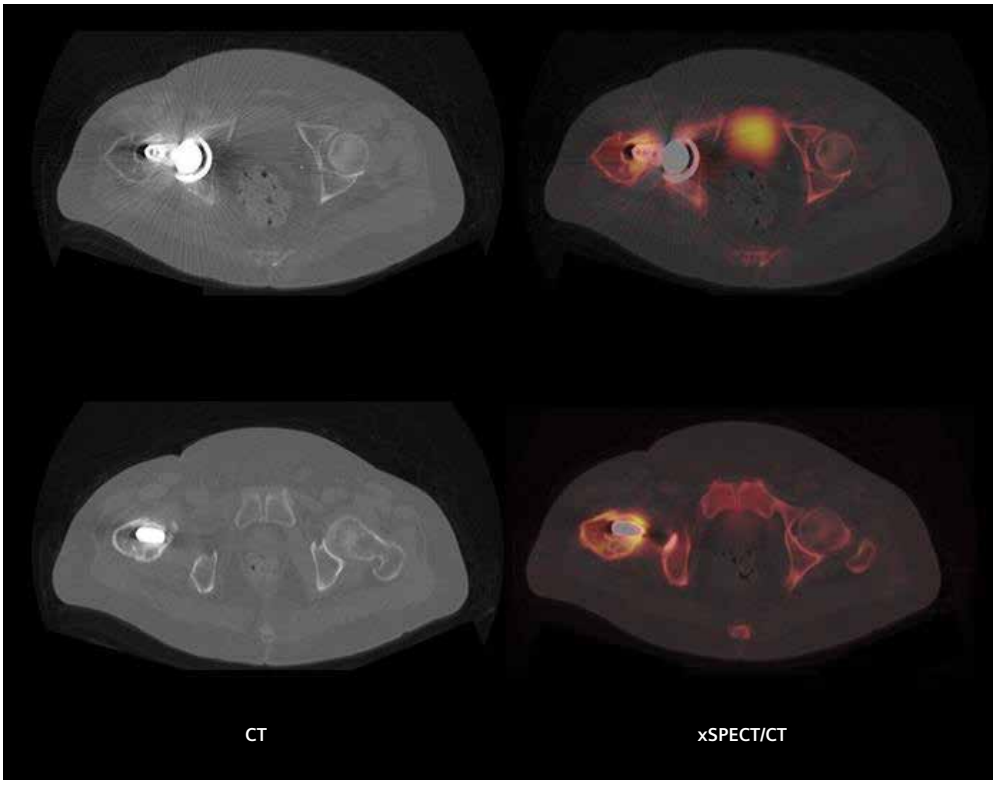

Figure 4: Axial slices through CT and fused CT and xSPECT Bone images at the level of the femoral head and lesser trochanter show absence of abnormal uptake around the acetabular cup, but increased uptake in the lesser trochanteric cortex that is adjacent to the stem of the femoral component of the prosthesis.

abnormal prosthetic movements, due to laxity of the joint. The CT findings of enlarged radiolucent zones at the interface of the prosthesis and bone (enlarged Gruen zones) also supported the diagnosis of prosthetic loosening.

Infection of the prosthetic joint often shows a diffuse increase in uptake around the prosthesis and infection imaging and scintigraphy using labelled leucocytes or other infection imaging agents are helpful in differentiation. In the present case, the xSPECT Bone study showed increased uptake throughout the stem, but there was clear visualization of enlarged Gruen zones and focal increase in the tip of the stem over and above the general hypermetabolism around the stem. These findings are more in favor of loosening, though infection imaging was requested to confirm absence of prosthetic infection.

Conclusion

xSPECT Bone showed sharp definition of periprosthetic uptake compared to standard 3D iterative reconstructions and clear visualization of the peri-implant radiolucent Gruen zones, which had even better definition on fused images. xSPECT Bone thus guides the radiologist towards the diagnosis of loosening which when confirmed would require revision arthroplasty. ■

Examination Protocol

Scanner: Symbia Intevo

SPECT	
Injected Dose	500 MBq (13.5 mCi) ^{99m}Tc MDP
Scan Delay	3 hours
Acquisition	32 stops, 20 sec/stop

CT	
Tube Voltage	130 kV
Tube Current	45 eff mAs
Slice Collimation	16 x 1.2 mm
Slice Thickness	2 mm

* Symbia Intevo and xSPECT Bone are not commercially available in all countries. Due to regulatory reasons their future availability cannot be guaranteed. Please contact your local Siemens organization for further details.

Case 3

Sharp Delineation of Loosening of Lumbar Vertebral Stabilization Screw with xSPECT Bone

By Partha Ghosh, MD, Molecular Imaging Business Unit, Siemens Healthcare

Data courtesy information on file

History

A 73-year-old female, who had a history of spinal surgery, underwent a spinal fusion performed at the L3-L4-L5 level. An anterior lumbar interbody fusion (ALIF) with interbody PEEK cage insertion in the L3-L4 and L4-L5 intervertebral disc space was performed along with bilateral insertion of posterior pedicle screws in the L3, L4 and L5 vertebrae. One year after the spinal fusion surgery, the patient still complained of persistent pain. Clinical possibilities included screw loosening, broken spinal screw or rod, or nerve root compression. The patient underwent ^{99m}Tc MDP bone SPECT/CT to evaluate the status of vertebral fusion. The study was performed 3 hours following an IV injection of 925 MBq (25 mCi) ^{99m}Tc MDP. A non-contrast diagnostic CT was performed, followed by SPECT acquisition (32 stops, 20 sec/stop). xSPECT Bone* reconstruction was performed using CT-based zone maps. xSPECT Bone reconstructions were fused with diagnostic CT for evaluation.

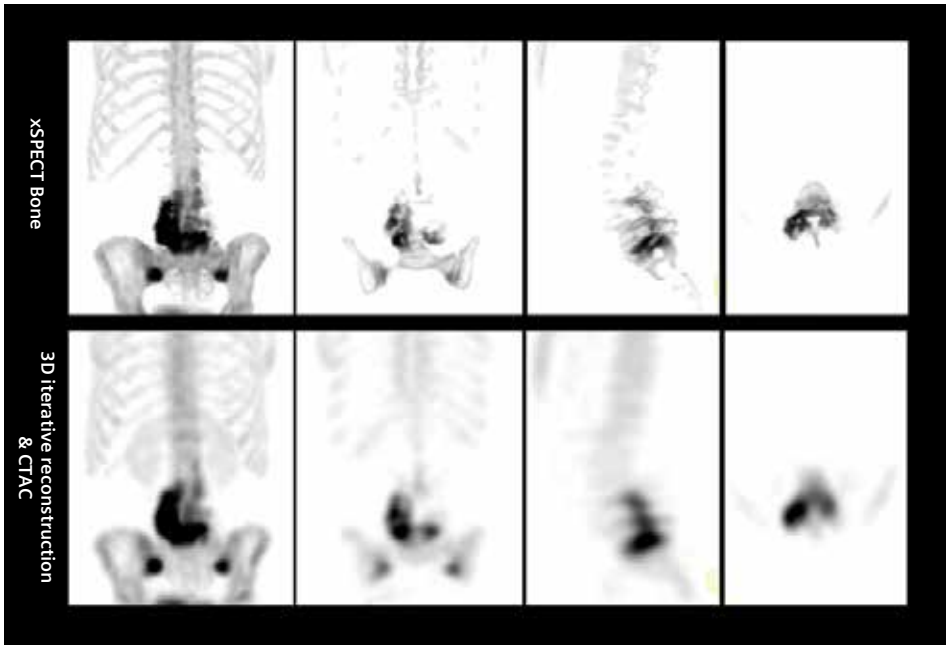

Figure 1: Anterior maximum intensity projection (MIP) and orthogonal multiplanar reconstruction (MPR) images of 3D iterative reconstruction and xSPECT Bone compared at similar slice levels show xSPECT Bone demonstrating sharper delineation of increased uptake of tracer around the shaft of the right lower spinal screw inserted to the body L5 vertebrae. The pattern of uptake strongly suggests loosening of the right side L5 screw. Uptake intensity is lower around the screws inserted to the right L4 and L3 vertebrae, suggesting the principal loosening was at the L5 level. The corresponding screws on the left side in the L3, L4 and L5 vertebras show much lower intensity of uptake, suggesting that instability secondary to loosening was primarily affecting the right side. xSPECT Bone sharply defines the shaft of the screws and the linear uptakes adjacent to the screws, which helps clearly localize the site and severity of stress reaction secondary to loosening.

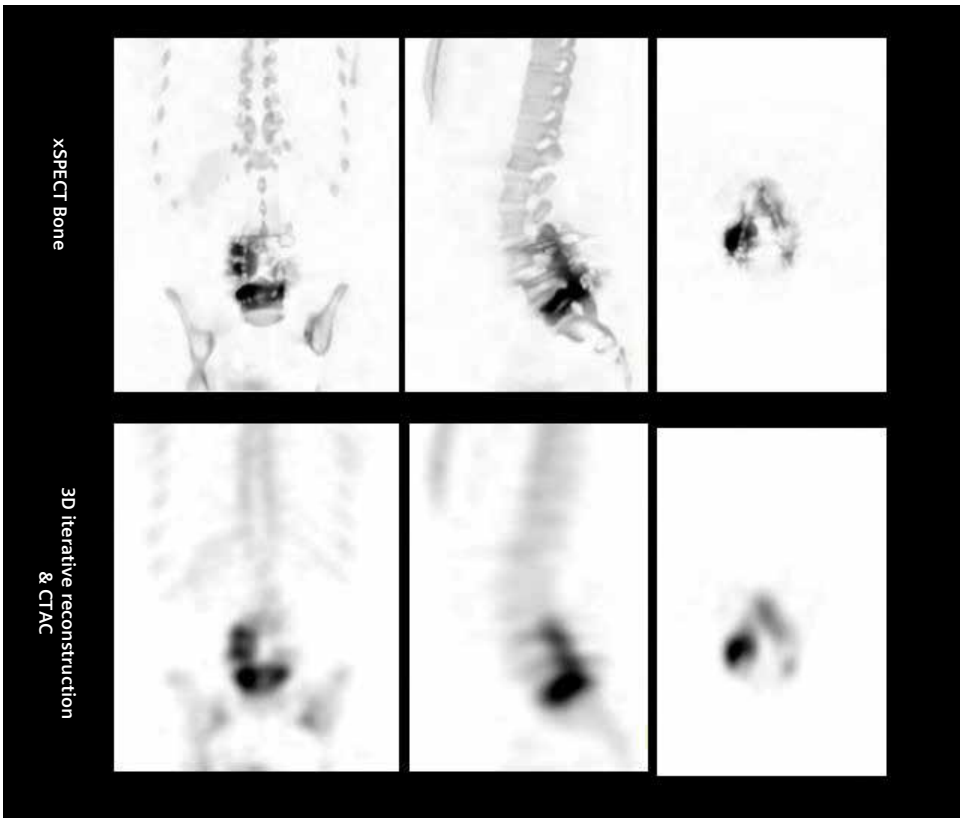

Figure 2: Comparison images at the level of the right-sided spinal screws and axial section through-screw in L4 vertebrae show linear increase in uptake throughout the entire length of the right L5 screw. However, the hypermetabolism is predominantly at the posterior end of the right L4 screw. This suggests principal loosening at the right L5 screw level, with reactive hypermetabolism due to instability arising from the loosening at the right L4 and L3 screw levels. xSPECT Bone shows sharper definition of uptake at the screw level along with clear outlines of the screw shaft.

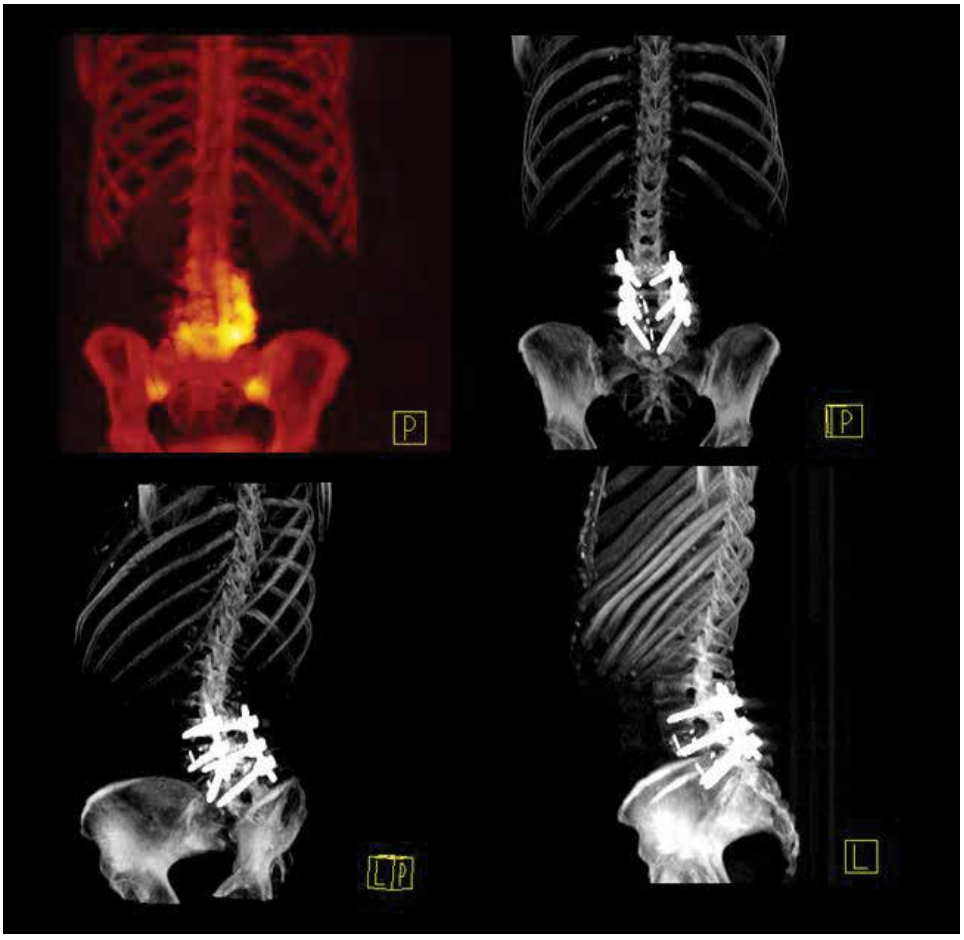

Figure 3: Posterior, oblique and lateral views of the MIP of xSPECT Bone and CT show the increased hypermetabolism and the corresponding right lower lumbar screw.

Figure 4: CT, xSPECT Bone and fused images show maximum hypermetabolism around the right L5 fixation screw, along with reactive hypermetabolism in the posterior ends of the right L4 fixation screw. Note the absence of significant uptake in the left L3 and L4 screws and only minor uptake in the left L5 spinal fixation screw, which reflects lower level of instability affecting the left-sided screws.

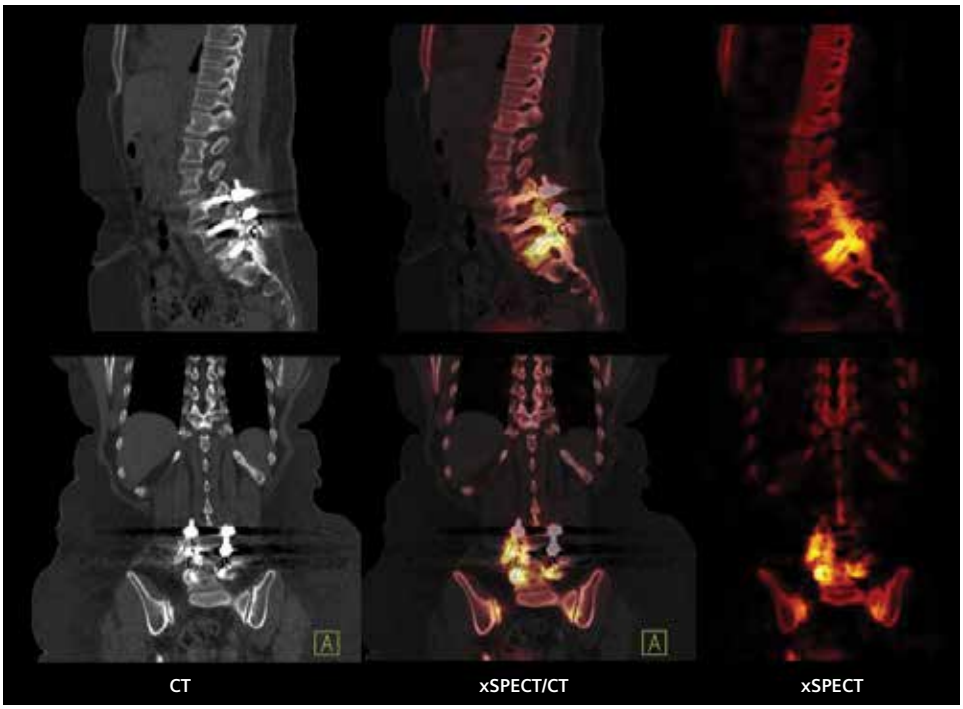

Figure 5: Posterior view of xSPECT Bone MIP shows increased uptake in the right-sided L5 screw along with reactive uptake in the right L4 and L3 screws. CT and fusion of CT and xSPECT Bone at different levels within the L5 vertebral body delineate the entire length of the right L5 screw and show periprosthetic linear increased uptake that is typical of loosening.

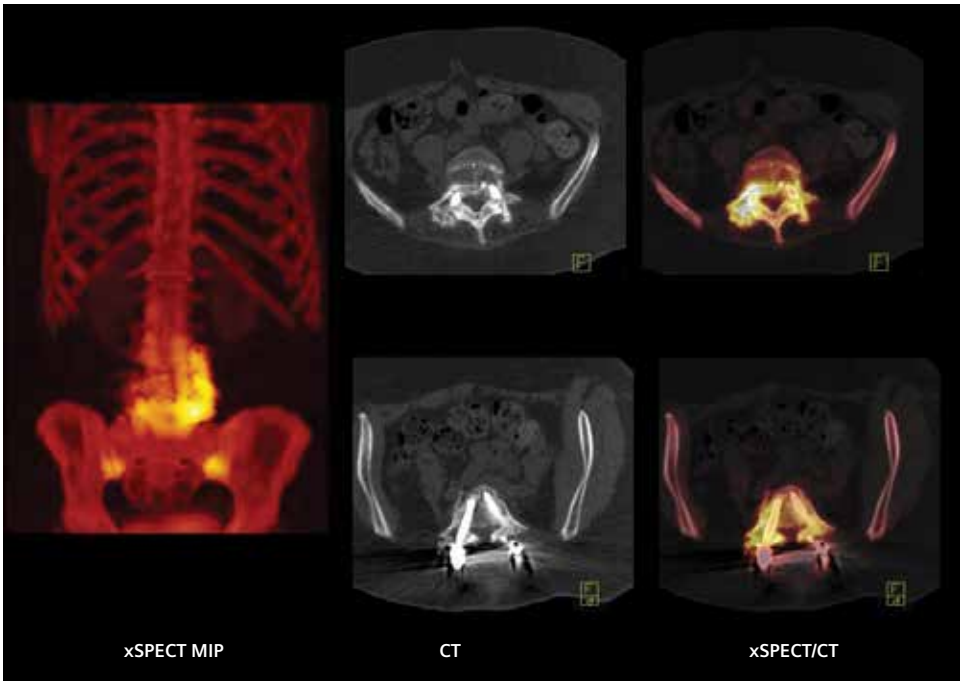

Diagnosis
As delineated by the CT and fused CT and xSPECT Bone images (*Figures 1-5*), the increased uptake of ^{99m}Tc MDP around the right L5 pedicular loosening of the screw, along with resultant instability of the L4-L5 vertebral interface at the articular facet levels, led to hypermetabolism in the posterior aspect of the right L4 screw as well. The interbody spacer between L4-L5 and L3-L4 did not show increased uptake, which suggested adequate fusion of adjacent vertebral bodies.

Compared to standard 3D iterative reconstruction, xSPECT Bone sharply defined the linear increase in uptake around the entire length of the right L5 screw along with highlighting the screw shaft, which suggested loosening. The uptake level and location at the posterior end of the right L4 screw was also reflective of the secondary effect of the resultant instability due to the L5 screw loosening. xSPECT Bone was helpful in sharp and exact localization of the increased uptake in the posterior end of the right L4 screw. The left-sided screws did not show increased uptake, except for that in the L5 vertebrae, which is a reactive change to the instability.

In view of the SPECT/CT findings, the patient was referred for re-surgery with modification of the spinal stabilization procedure with bone grafting.

Comments
Bone SPECT/CT is uniquely suited to evaluate failure of spinal fusion and assess prosthetic loosening, infections, instability stress and fractures. Rager et al.[1] performed bone SPECT/CT in 10 patients with failed lumbar fusion with recurrence of back pain and suspicion of pseudoarthrosis on conventional imaging. The presence of screw-loosening, the non-union around the intervertebral disc cage or spacers, and the facet joint degeneration were all assessed for pseudoarthrosis. Screw-loosening seen on CT was always associated with abnormal uptake on SPECT/CT. Non-union around the intervertebral disc cages seen on CT was often not associated with hypermetabolism, which reflected failure of bone graft functioning. SPECT/CT was far more accurate than CT in defining facet joint hypermetabolism related to vertebral instability. Based on SPECT/CT, 6 of 10 patients underwent surgical re-intervention.

In another study involving 37 patients suffering from lower back pain after lumbar fusion surgery,[2] SPECT/CT reclassified 45% of the cases when compared with planar and SPECT bone scintigraphy. The reclassification rate was nearly 50% for patients diagnosed as metal loosening and insufficient stabilizing function of the metal implants indicated by metabolically active facet joint arthritis and/or intervertebral osteochondrosis. The authors concluded that SPECT/CT should be the procedure of choice for evaluation of back pain following lumbar fusion.

Conclusion
In the present case, there was periprosthetic lucency around the right L5 screw seen on CT, more towards the posterior aspect which was suggestive of loosening. However, the pattern and intensity of hypermetabolism involving the entire length of the screw shaft was typical of loosening and reflected the extent of instability as well as the effect on the adjacent screws in L4 and L3 vertebrae. xSPECT Bone in combination with diagnostic CT thus provided comprehensive information on the morphological and functional impact of the loosening of the spinal stabilization screw and helped guide surgical intervention. ■

Examination Protocol

Scanner: Symbia Intevo™*

SPECT	
Injected Dose	925 MBq (25 mCi) ^{99m}Tc MDP
Scan Delay	3 hours
Acquisition	32 stops, 20 sec/stop

CT	Non-contrast diagnostic
Tube Voltage	110 kV
Tube Current	100 eff mAs
Slice Collimation	16 x 1.2 mm
Slice Thickness	2 mm

References:
[1] Rager et al. *Clin Nucl Med*. 2012, Apr. 37(4): 339-343.
[2] Sumer et al. *Nucl Med Commun*. 2013, Oct. 34(10) : 964-970.

* Symbia Intevo and xSPECT Bone are not commercially available in all countries. Due to regulatory reasons their future availability cannot be guaranteed. Please contact your local Siemens organization for further details.

Case 4

Delineation of Periprosthetic Fissure in a Patient with Intramedullary Nail Implantation Using xSPECT Bone

By Christian Waldherr, MD, and Martin Sonnenschein, MD

Data courtesy of the Department of Radiology & Nuclear Medicine, Klinik Engeried, Bern, Switzerland

History
A 45-year-old man with a history of intramedullary nail implantation presented with pain in the mid-thigh. Clinical suspicion included broken nail or loosening. Periprosthetic fracture or infection also were suggested as possibilities. X-rays did not show significant cortical abnormality. In view of a possible periprosthetic fracture, a 3-phase bone scintigraphy, followed by a SPECT/CT of the foot was performed on a Symbia Intevo™* scanner.

Initial planar dynamic and blood pool images were acquired immediately following an IV injection of 600 MBq (16.22 mCi) ^{99m}Tc MDP. Planar whole-body and SPECT/CT acquisition of the thigh were performed 3 hours post injection. Following a thin slice diagnostic CT (110 kV, 120 mAs CareDose) SPECT was acquired with 32 stops per detector at 20 sec/stop. xSPECT Bone* reconstruction was performed using CT-based zone information. xSPECT Bone data was fused with the CT for a final evaluation.

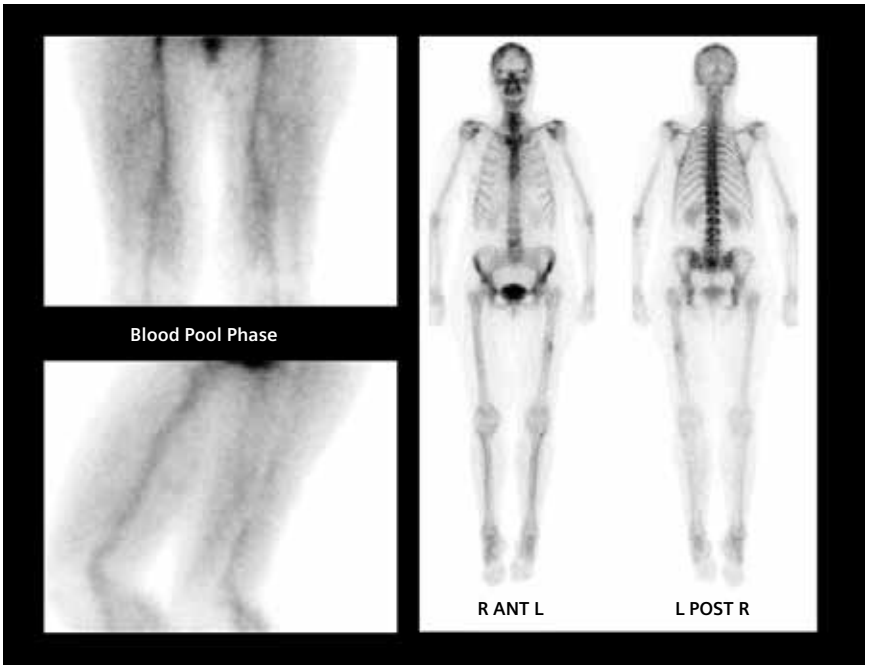

Figure 1: Initial blood pool images show no abnormal blood pool activity in the thigh. Delayed planar images show a focal area of mildly increased uptake in the lateral aspect of the cortex of the middle left femur.

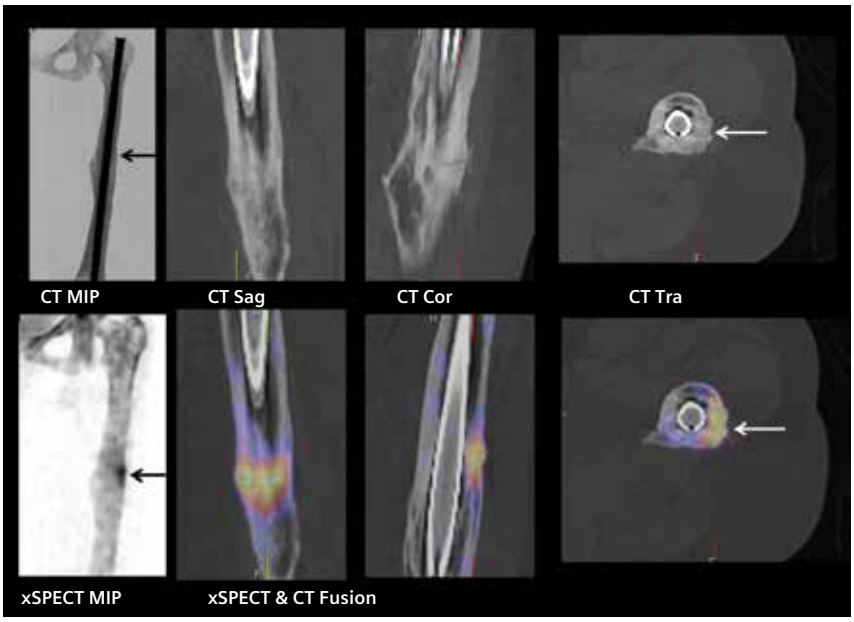

Figure 2: xSPECT Bone maximum intensity projection (MIP) shows a focal area of increased uptake in the lateral cortex of the middle of the shaft of the left femur. CT shows irregular callus formation in the involved femoral cortex (*arrows*). xSPECT- and CT-fused images show increased uptake of tracer that exactly corresponds to the slightly radiodense callus formation. The pattern of uptake and CT findings suggest a healing subacute periprosthetic fissure.

Diagnosis
Initial dynamic images showed an absence of significant blood pool activity, thereby ruling out infection. xSPECT Bone and CT findings suggested a subacute periprosthetic fissure in the lateral cortex of the middle shaft of the left femur, possibly created due to cortical stress during implantation of the intramedullary nail. The degree of callus formation in the lateral cortex suggested significant healing of the fissure. There was an absence of tracer uptake in the end of the intramedullary nail or along the nail shaft, which suggested an absence of osseous stress associated with loosening. The absence of significant radiolucency between the margin of the intramedullary nail and the adjacent cortex also suggested an absence of significant loosening. The intramedullary nail appeared intact. There was no soft tissue abnormality seen on CT around the femur. xSPECT Bone and fused images confirmed the presence of healing periprosthetic fissure, and ruled out other potential considerations like loosening or infection. In view of the active healing of the fissure determined on SPECT/CT, the patient was treated conservatively.

Comments
Periprosthetic fissures are cracks in the bony cortex, commonly arising in the shaft of long bones during rasping of the medullary canal prior to prosthesis insertion. As the prosthesis is inserted, these fissures gape open. Cemented prosthesis implantation may lead to penetration of cement within these fissures, which can permanently prevent repair and remodeling of the fissure. When an uncemented prosthesis is used, spontaneous healing of the bony crack with callus formation usually occurs, resulting in closure of the fissure by 6 months following the prosthesis insertion. In the present case, the degree of healing of the fissure shown by the callus formation at the fissure site reflected the uncemented nature of the intramedullary nail insertion.

Conclusion
xSPECT bone showed sharp delineation of focal cortical uptake at the fissure site, which co-registered exactly with the callus on CT. Improved definition of cortical uptake with xSPECT Bone should help earlier detection of such lesions. ■

Examination Protocol

Scanner: Symbia Intevo

SPECT	
Injected Dose	600 MBq (16.22 mCi) ^{99m}Tc MDP
Scan Delay	3 hours
Acquisition	64 projections, 20 sec/stop

CT	Non-contrast diagnostic
Tube Voltage	110 kV
Tube Current	120 eff mAs
Slice Collimation	16 x 2.5 mm
Slice Thickness	3 mm

* Symbia Intevo and xSPECT Bone are not commercially available in all countries. Due to regulatory reasons their future availability cannot be guaranteed. Please contact your local Siemens organization for further details.

Case 5

Delineation of Pseudoarthrosis Secondary to Sacrococcygeal Fracture by xSPECT Bone

By Christian Waldherr, MD, and Martin Sonnenschein, MD

Data courtesy of the Department of Radiology & Nuclear Medicine, Klinik Engeried, Bern, Switzerland

History
A 45-year-old man presented with long-standing sacral pain. The pain began after the patient fell on his back. X-rays and MRI did not reveal any abnormal findings. The patient underwent ^{99m}Tc MDP bone SPECT/CT performed on a Symbia Intevo™* scanner. Planar whole-body and SPECT/CT acquisition of pelvis was performed 3 hours post injection (600 MBq [16.22 mCi] ^{99m}Tc MDP). Following a thin-slice diagnostic CT (110 kV, 120 mAs CareDose), SPECT was acquired with 32 stops per detector at 20 sec/stop. xSPECT Bone* reconstruction was performed using CT-based zone information. xSPECT Bone data was fused with the CT for a final evaluation.

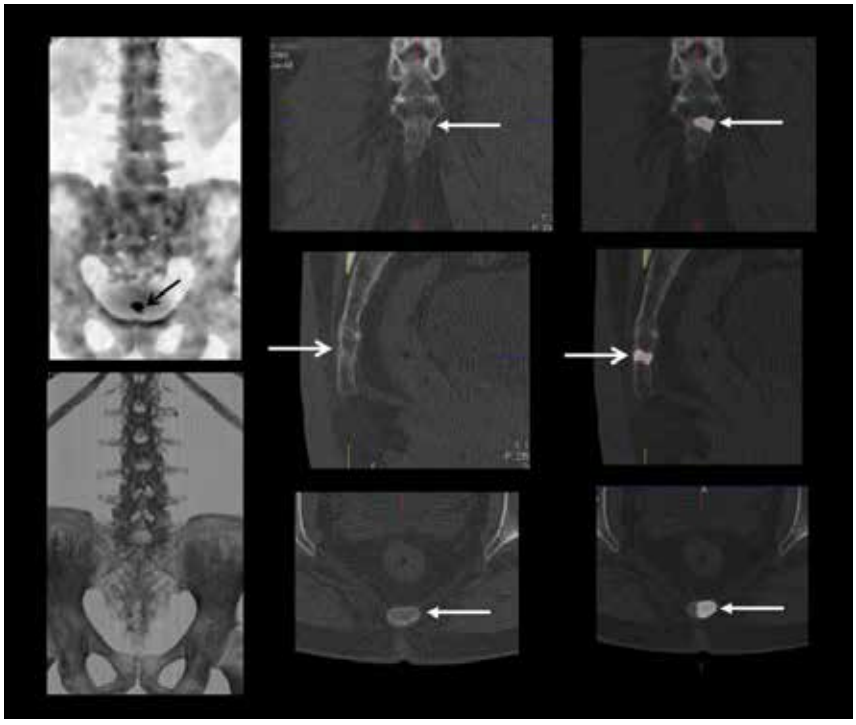

Figure 1: Maximum intensity projection (MIP) of xSPECT Bone shows focal area of intense uptake of ^{99m}Tc MDP in the coccyx (*black arrow*). CT images show a fracture involving the entire antero-posterior dimension of the coccyx with associated sclerosis (*white arrows*), with intense hypermetabolism, at the fracture site on the fused images. xSPECT Bone fused with CT shows exact co-registration of the focal uptake to the coccygeal margins. The uptake is also predominantly to the left, but crossing the mid-line, as seen in the coronal and axial fused images, which suggests a partial coccyx fracture following the fall. The intensity of the uptake and its location at the middle of the coccyx suggests pseudoarthrosis of a non-dislocated coccygeal fracture.

Figure 2: Sagittal reconstruction of thin-slice CT shows oblique fracture line through the mid-coccyx, with mild sclerosis at the fracture line. Fusion of xSPECT Bone and CT shows focal hypermetabolism exactly at the fracture line, with highest uptake intensity posteriorly.

Examination Protocol

Scanner: Symbia Intevo

SPECT	
Injected Dose	600 MBq (16.22 mCi) ^{99m}Tc MDP
Scan Delay	3 hours
Acquisition	64 projections, 20 sec/stop

CT	Non-contrast diagnostic
Tube Voltage	110 kV
Tube Current	120 eff mAs
Slice Collimation	16 x 2.5 mm
Slice Thickness	3 mm

* Symbia Intevo and xSPECT Bone are not commercially available in all countries. Due to regulatory reasons their future availability cannot be guaranteed. Please contact your local Siemens organization for further details.

The statements by Siemens customers described herein are based on results that were achieved in the customer's unique setting. Since there is no "typical" hospital and many variables exist (e.g., hospital size, case mix, level of IT adoption) there can be no guarantee that other customers will achieve the same results.

Diagnosis
CT showed a well-delineated, slightly oblique fracture of the coccyx at its middle, and with mild sclerosis at the fracture site. The fusion of xSPECT Bone and CT showed intense hypermetabolism, which exactly matched the fracture site, predominantly to the left, and suggested a partial coccygeal fracture with pseudoarthrosis—which caused increased bone turnover at the fracture site associated with pain. In absence of any other bony or soft tissue pathology, the diagnosis was that of pseudoarthrosis of a non-displaced coccygeal fracture. The patient was referred for local analgesic and glucocorticoid injection.

Comments
Pain in the coccyx (coccydynia) is an uncommon case of pain following falls on the back. Sacrococcygeal dislocation and coccygeal fracture are common causes. In the present case, a fracture involving the mid-coccyx led to formation of pseudoarthrosis with abnormal movement of one coccygeal fragment against another, leading to intense skeletal hypermetabolism visualized on the xSPECT Bone images.

Conclusion
xSPECT Bone showed sharp definition of focal coccygeal uptake with high contrast, along with sharp delineation of the sacral and lumbar spine uptake. Exact co-registration of the CT and xSPECT Bone at the margins of the coccygeal fracture visualized on the fused images reflected the high resolution of xSPECT Bone. ■

Case 6

Evaluation of Infection in Tibial Fracture Site with ^{99m}Tc-labelled Antigranulocyte Antibodies and SPECT/CT with xSPECT Quant

By Partha Ghosh, MD, Molecular Imaging Business Unit, Siemens Healthcare

Data courtesy of the Department of Nuclear Medicine, Bundeswehrkrankenhaus Ulm, Ulm, Germany

History
A 74-year-old female had an open comminuted fracture of the upper left part of the tibia. The fracture was treated with surgical reduction and internal fixation. Flap reconstruction surgery was performed on the surface wound. The tibial plateau fracture was treated with internal fixation using a dual plate. Prior to surgery, the patient experienced persistent pain, wound discharge and non-union of the fracture fragments. Suspicious of osteomyelitis of the tibial fracture fragments, the patient underwent infection imaging using ^{99m}Tc-labelled antigranulocyte antibodies and SPECT/CT. The study was performed on Symbia Intevo™*, using xSPECT Quant* for absolute quantification of tracer uptake.

760 MBq (20.54 mCi) of ^{99m}Tc antigranulocyte antibodies (Fab' sulesomab; antigen NCA-90) were injected. Initial dynamic and planar blood pool acquisitions were performed. SPECT/CT acquisition was performed at 1, 5 and 24 hours following the injection. Low-dose diagnostic CT was performed, followed by SPECT acquisition (32 stops per detector, 30 sec/stop). xSPECT Quant reconstructions were fused for evaluation. SUV_{max} values were obtained using xSPECT Quant and were compared across 5- and 24-hour acquisitions.

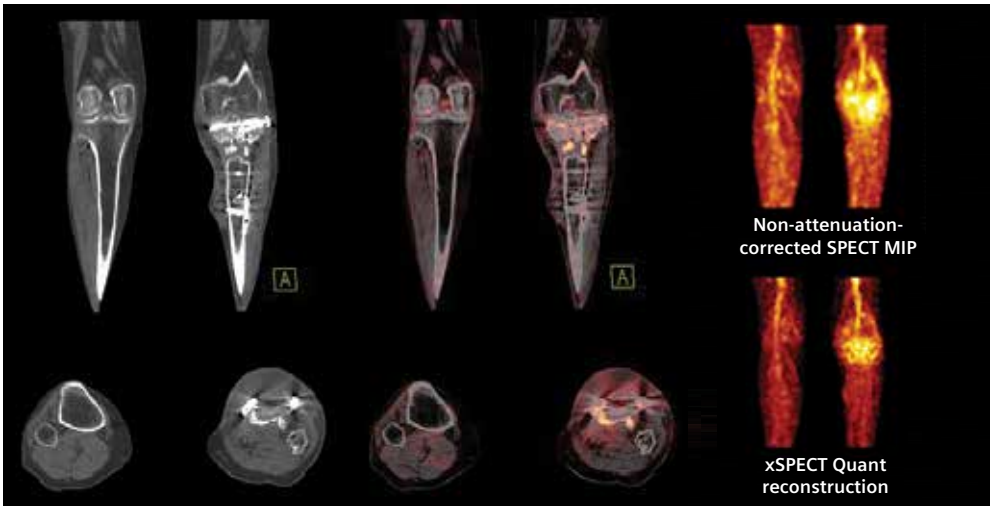

Figure 1: CT and fused SPECT/CT images show multiple inhomogeneous focal areas of accumulation of ^{99m}Tc-labelled antigranulocyte antibodies within the tibial head, which corresponds with the small sclerotic bone fragments and metal plates of the internal fixation device (especially the plate passing through the upper end, just below the tibial condylar surfaces and intercondylar cleft). CT demonstrates small fracture fragments within the upper end of the tibia with internal fixation plates.

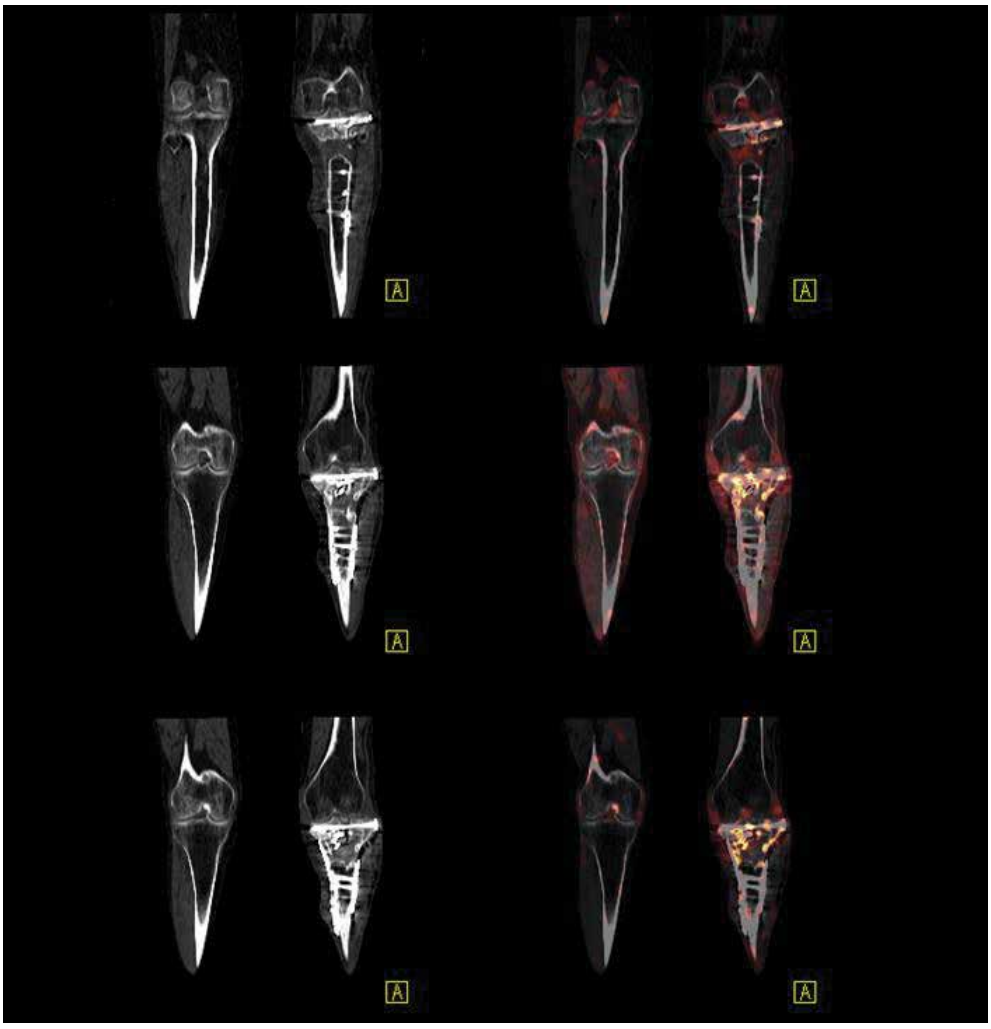

Figure 2: Coronal CT and fused SPECT/CT slices demonstrate the extent of accumulation of ^{99m}Tc-labelled antigranulocyte antibodies within the tibial plateau, fracture fragments and internal fixation plates—which suggests an active infection.

Diagnosis

SPECT/CT images (*Figures 1-3*) showed focal areas of intense inhomogeneous accumulation of ^{99m}Tc-labelled antigranulocyte antibodies within the fracture fragments, in the proximal end of the left tibia and the internal fixation plates (especially the intercondylar plate). The uptake pattern suggested an active osteomyelitis. Absolute quantification of tracer uptake on SPECT was performed using xSPECT Quant, and the SUV_{max} of different focal areas of tracer uptake were compared across the 5- and 24-hour SPECT/CT acquisitions.

Two main focal areas of uptake within the tibial plateau fracture (*Figure 4*) showed an SUV_{max} of 2.12 and 2.61, respectively, in the study performed 5 hours after tracer injection. In the study acquired 24 hours following tracer injection, the SUV_{max} increased to 4.43 and 4.56, respectively. This significant increase suggested a progressive accumulation of radiolabelled antigranulocyte antibodies and reflected an active infection (osteomyelitis).

Due to the active osteomyelitis, the patient underwent a revision arthroplasty with complete removal of all metal internal fixation plates; resection of the majority of the proximal tibia, including the condyles; and replacement of the proximal tibia, using a gentamicin impregnated bone cement spacer and an external fixation of the femoral and tibial shafts. Once the bone was no longer infected, a delayed arthrodesis was planned. Microbiological evaluation of the resected tibial bone fragment demonstrated propionibacterium acnes infection.

Comments

Scintigraphic imaging for a bone infection with radiolabelled leucocytes or ^{99m}Tc-labelled antigranulocyte antibodies has been widely used. With improved localization of infective foci, SPECT/CT has shown to be effective. ^{99m}Tc-labelled leucocyte SPECT/CT demonstrated 87% sensitivity and 71% specificity in demonstrat-

ing osteomyelitis in patients with diabetic foot ulceration.[1] Since leucocytes migrate to sites of infection, there is a rationale for comparing intensity of radiolabelled leucocyte accumulation between early (4- to 6-hour) and late (20- to 24-hour) images with the expectation that active infection would show progressive increase in uptake intensity. Larikka et al.[2] demonstrated higher sensitivity, specificity and positive predictive value of late (24 hours) imaging with ^{99m}Tc HMPAO-labelled leucocytes in 64 patients with suspected infection in hip prosthesis. Late infection imaging showed a sensitivity of 83% and specificity of 100% compared to that of early imaging (sensitivity 50%; specificity 90%).

In this patient, there was a visual increase in uptake-intensity at the infection site in the proximal tibia between the 5- and 24-hour image. However, SUV_{max} obtained with xSPECT Quant demonstrated quantitative increases in uptake intensity of more than 100%. For example, SUV_{max} in one infective foci increased from 2.12 at 5 hours to 4.43 at 24 hours.

Conclusion

The xSPECT Quant method of absolute quantification of tracer uptake is new to SPECT and proves to be a valuable technique supporting the diagnosis of infections as well as help assess therapy response. ■

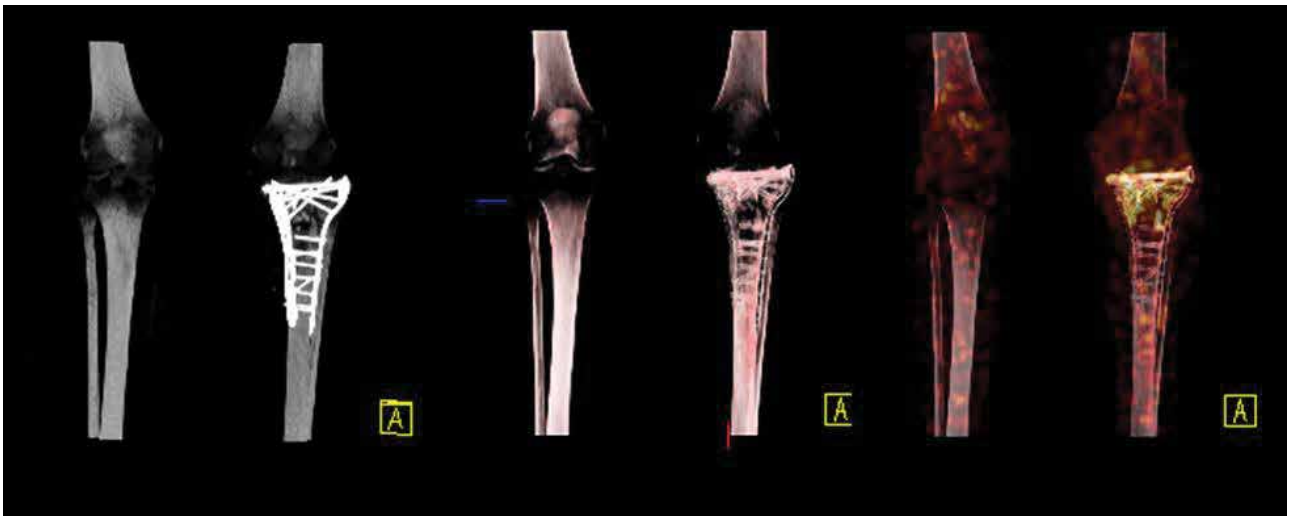

Figure 3: SPECT maximum intensity projection (MIP) and a volume rendering of CT show the dual plates of the internal fixation holding multiple fracture fragments in the tibia's upper end. Volume rendering of fused SPECT/CT shows intense uptake of ^{99m}Tc-labelled antigranulocyte antibodies in the region of the fracture fragments and internal fixation plates. This suggests an active infection throughout the entire proximal end of the tibia.

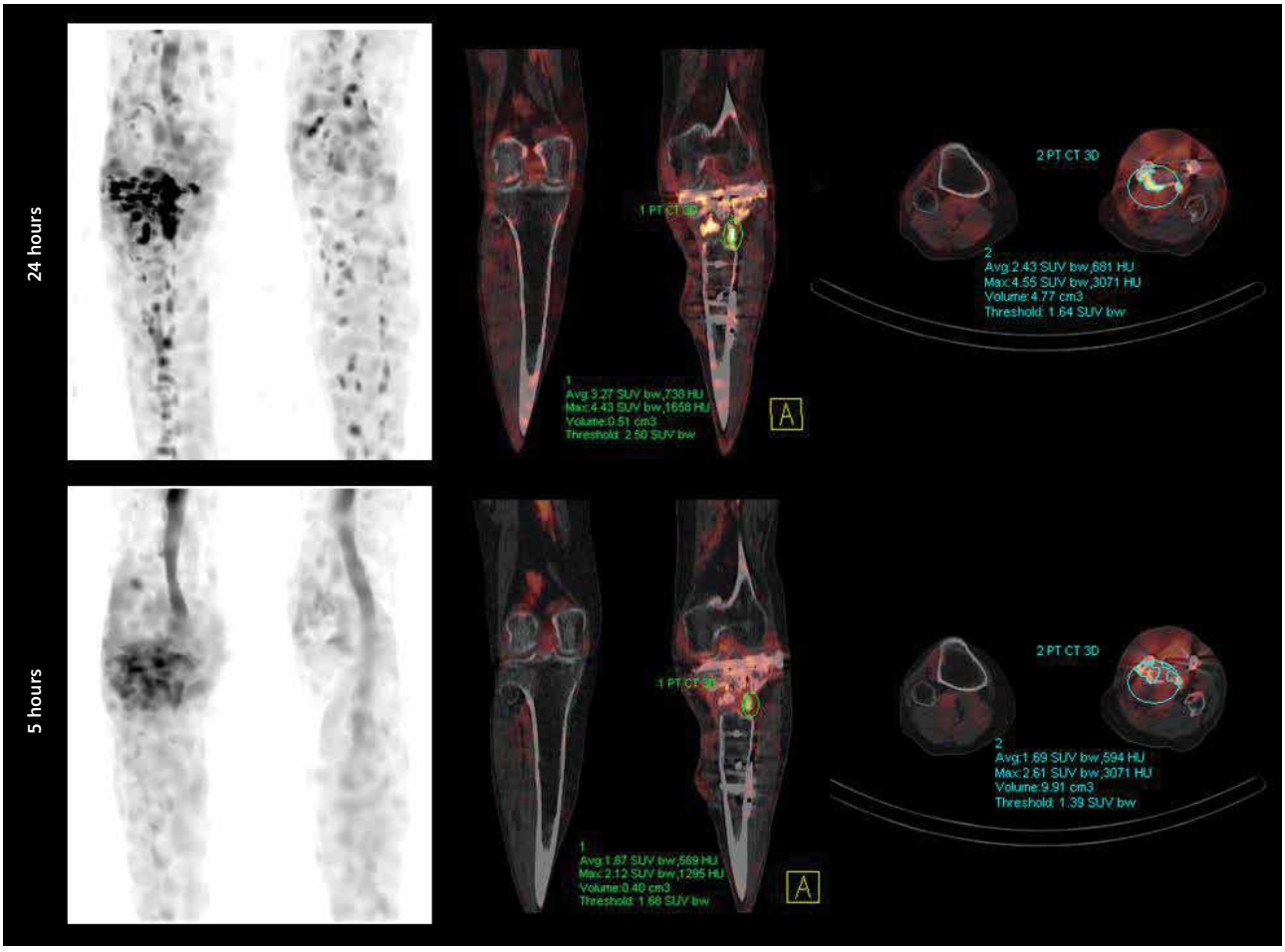

Figure 4: SUV_{max} comparison of uptake in the proximal end of the left tibia between 5- and 24-hour acquisitions shows a significant increase in SUV_{max} with time.

Examination Protocol

Scanner: Symbia Intevo

SPECT	
Injected Dose	20.54 mCi (760 MBq) ^{99m}Tc antigranulocyte antibodies
Scan Delay	5 & 24 hrs post injection
Acquisition	64 projections, 30 sec/stop

CT	
Tube Voltage	130 kV
Tube Current	17 eff mAs
Slice Collimation	16 x 1.2 mm
Slice Thickness	2 mm

References:
[1] Przybylski et al. *Int Wound J*. 2014, Jun 26.
[2] Larikka et al. *EJNM*. 2001. 28: 288-293.

* Symbia Intevo and xSPECT Quant are not commercially available in all countries. Due to regulatory reasons their future availability cannot be guaranteed. Please contact your local Siemens organization for further details.

Case 7

Tear of Acetabular Labrum Delineated with xSPECT Bone

By Xuan Pham, MD, and François Raymond, MD

Data courtesy of CSSS de Gatineau, Hôpital de Hull, Hull, Canada

History

A 24-year-old soccer player presented with pain in the right hip and groin. X-rays did not show a clearly defined abnormality. Therefore, the patient underwent a ^{99m}Tc MDP bone SPECT/CT to define active pelvic skeletal pathology. The study was performed on a Symbia Intevo™* 16 scanner, 3 hours following an IV injection of 13.5 mCi (500 MBq) of ^{99m}Tc MDP. A low-dose CT study was followed by the SPECT study, using 32 stops at 20 sec per stop. xSPECT Bone* reconstructions were performed using CT-based zone maps.

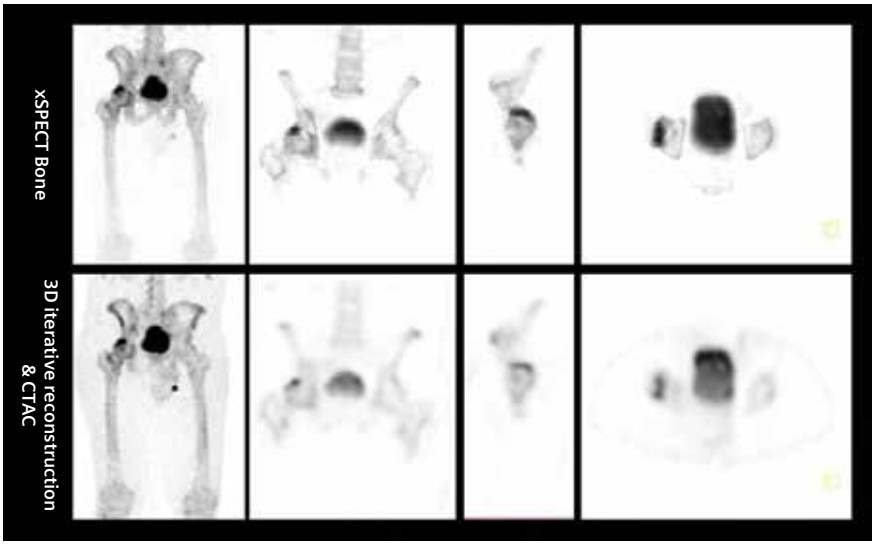

Figure 1: Comparison images of maximum intensity projection (MIP) and multiplanar reconstruction (MPR) images of 3D iterative reconstruction and xSPECT Bone show increased contrast and sharper definition of focal uptake in the right acetabular labrum. The cortical uptake in the femoral head, neck and trochanter, acetabular margins, and the iliac crest is sharply defined on xSPECT Bone, when compared to standard 3D iterative reconstructions.

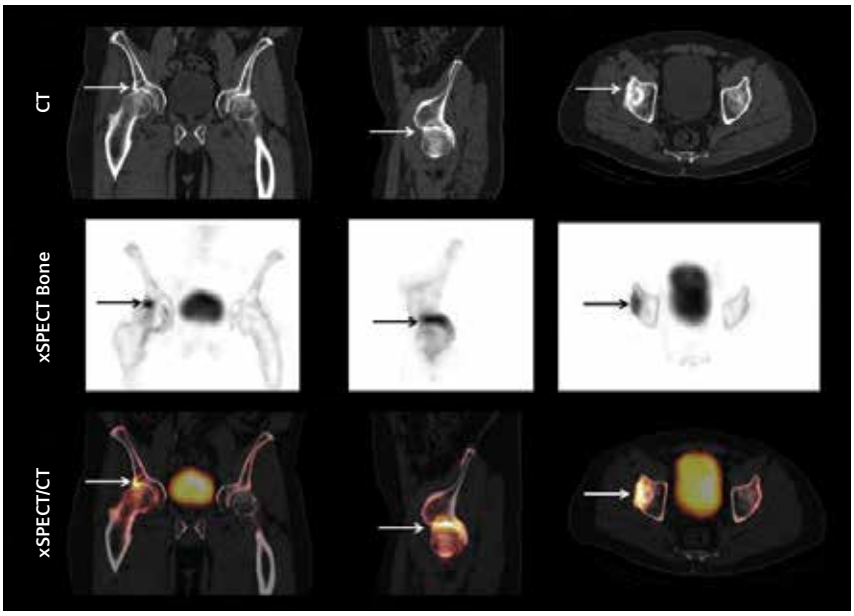

Figure 2: CT, xSPECT Bone and fused CT and xSPECT Bone show increased uptake of tracer in the right acetabular labrum (*arrows*), which also shows irregularities in the acetabular margin and small bony fragments of the acetabular labrum, suggestive of an acetabular labral tear.

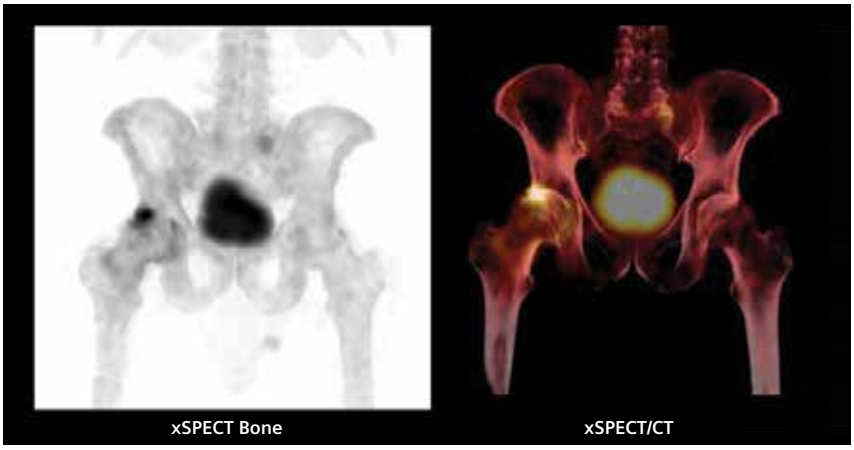

Figure 3: MIP of xSPECT Bone and volume rendering of xSPECT/CT data show focal uptake of ^{99m}Tc MDP at the antero-superior aspect of the acetabulum and the adjacent anterolateral femoral head. The contralateral acetabulum appears normal.

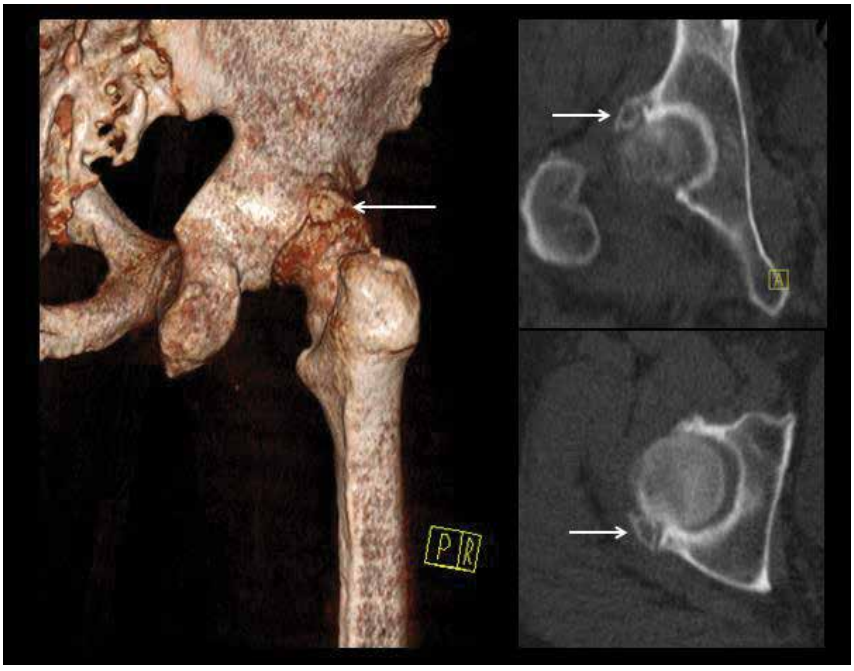

Figure 4: Coronal and axial CT and volume rendering of the hip joint shows fragment of acetabular labrum, clearly defining the labral tear.

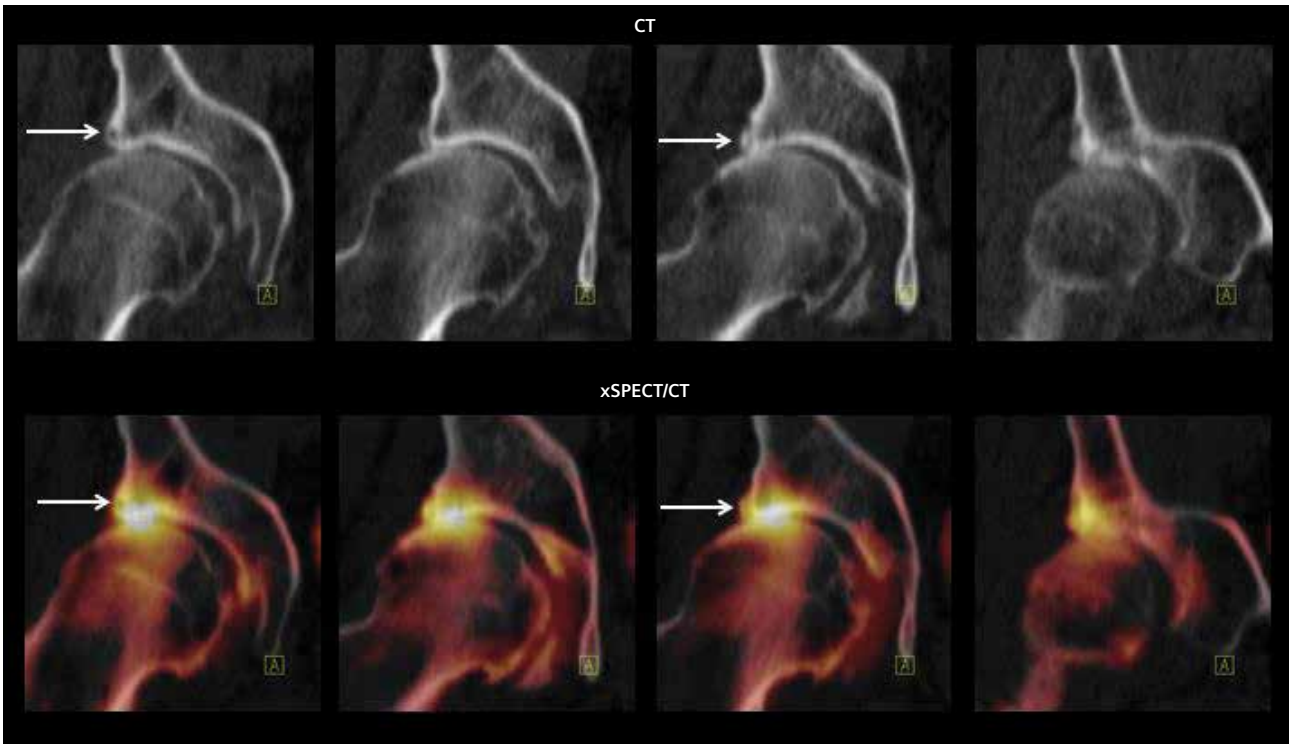

Figure 4: Serial coronal slices of CT and fusion of CT and xSPECT Bone show a tear of the right acetabular labrum and corresponding hypermetabolism in the torn acetabular labrum and adjacent femoral head. The CT images show femoro-acetabular impingement of the cam type, with the superior acetabular labral edge impinging on the adjacent superior femoral head surface with resultant localized hypermetabolism.

Diagnosis

The CT showed a tear of the acetabular labrum with the torn labral fragment clearly defined on CT separate from the labral margin (*Figures 4 & 5, arrows*). The CT appearance of the labral tear suggested that it was a type I tear,[1] the detachment of the labrum from the articular surface occurring at the transition zone between the fibrocartilage of the labrum and the articular cartilage. Some cystic spaces within the labral fibrocartilage were also visualized on CT.

The CT image suggested a femoro-acetabular impingement of the right hip with the free edge of the antero-superior acetabular labrum impinging onto the adjacent femoral head. In this patient, the repeated impingement of the labral edge on the femur's head, due to hip joint movement, was the cause of the acetabular labral tear. Fused CT and xSPECT Bone clearly demonstrated the tear and the functional impact related to hypermetabolism in the tear and in the site of impingement, the adjacent femoral head.

The patient was referred for an arthroscopic repair of the torn acetabular labrum.

Comments

Hip pain in young adults, especially those involved in sports, is commonly associated with acetabular labral tears. 80% of acetabular labral tears are associated with femoro-acetabular impingement[2] in which the free edge of the acetabular labrum cannot glide over the adjacent femoral head, but impinges on it. The impingement usually happens because the labrum is either too short to adequately cover the larger abnormally shaped femoral head (cam impingement), or too long, so as to over cover the femoral head and create abnormal contact with the femoral neck with extreme rotation of the hip (pincer impingement).

The patient in this study appeared to have a cam impingement, as seen on the CT. A tear of the labrum is related

to repeated impingement with extreme hip rotation, which is likely in a soccer player, and leads to avulsion of the labrum from the acetabular articular cartilage. SPECT/CT is sensitive in detecting acetabular labral lesions related to femoro-acetabular impingement. Matar et al.[2] evaluated 25 patients using ^{99m}Tc MDP bone SPECT—all of whom were suspected for femoro-acetabular impingement because each had hip pain for over 6 months and demonstrated signs of positive impingement and radiographic evidence, including α angle higher than 65 degrees. A positive SPECT scan was defined as increased uptake at the antero-superior aspect of acetabulum, the adjacent femoral head and femoral head/neck junction. SPECT was 84.7% sensitive and 62.5% specific in identifying femoro-acetabular impingement. A final diagnosis was based on radiographic and clinical findings. In some patients the contralateral hip also showed acetabular hypermetabolism without any symptoms, and in one patient, the contralateral hip developed progressive pain. Therefore, SPECT was also able to identify pre-symptomatic femoro-acetabular impingement in the contralateral hip.

Conclusion

xSPECT Bone clearly and sharply defined the focal hypermetabolism in the labrum, which exactly corresponded to the region of the labral tear in the antero-superior free edge and the adjacent femoral head impinging on the labrum. xSPECT Bone demonstrated higher contrast and sharper definition of the uptake in the labral tear and adjacent femoral head surface compared to standard 3D iterative reconstructions. The definition of the uninvolved bone including the rest of the acetabular surface, femoral head and neck, and iliac crest was much sharper, demonstrating higher resolution and clear definition of skeletal metabolic activity with xSPECT Bone, compared to 3D iterative reconstruction. Fusion of CT and xSPECT Bone was also exact with perfect co-registration of the labral tear with increased uptake, thereby confirming the impact of the impingement and labral tear. ■

Examination Protocol

Scanner: Symbia Intevo

SPECT	
Injected Dose	500 MBq (13.5 mCi) ^{99m}Tc MDP
Scan Delay	3 hours
Acquisition	32 stops, 20 sec/stop

CT	
Tube Voltage	130 kV
Tube Current	45 eff mAs
Slice Collimation	16 x 1.2 mm
Slice Thickness	2 mm

References:
[1] Seldes et al. *Clin Orthop*. 2001; 382: 232–240.
[2] Matar et al. *Clin Orthop Relat Res*. 2009; 467: 676–681.

* Symbia Intevo and xSPECT Bone are not commercially available in all countries. Due to regulatory reasons their future availability cannot be guaranteed. Please contact your local Siemens organization for further details.

Case 8

Delineation of Pathological Fracture in Lower End of Femur Using xSPECT Bone

By Partha Ghosh, MD, Molecular Imaging Business Unit, Siemens Healthcare

Data courtesy of Associate Prof. Michael Hofman, Peter MacCallum Cancer Centre, Melbourne, Australia

History
A 62-year-old female with newly diagnosed breast carcinoma underwent a ^{99m}Tc MDP bone scan for initial staging. Since there was abnormal uptake in the knee joint, the SPECT/CT study followed the initial planar images. The study was performed on a Symbia Intevo™* 16 scanner, 3 hours following an IV injection of 20 mCi (740 MBq) of ^{99m}Tc MDP. A low-dose CT study was followed by the SPECT study, using 32 stops at 20 sec/stop. xSPECT Bone* reconstructions were performed using CT-based zone maps.

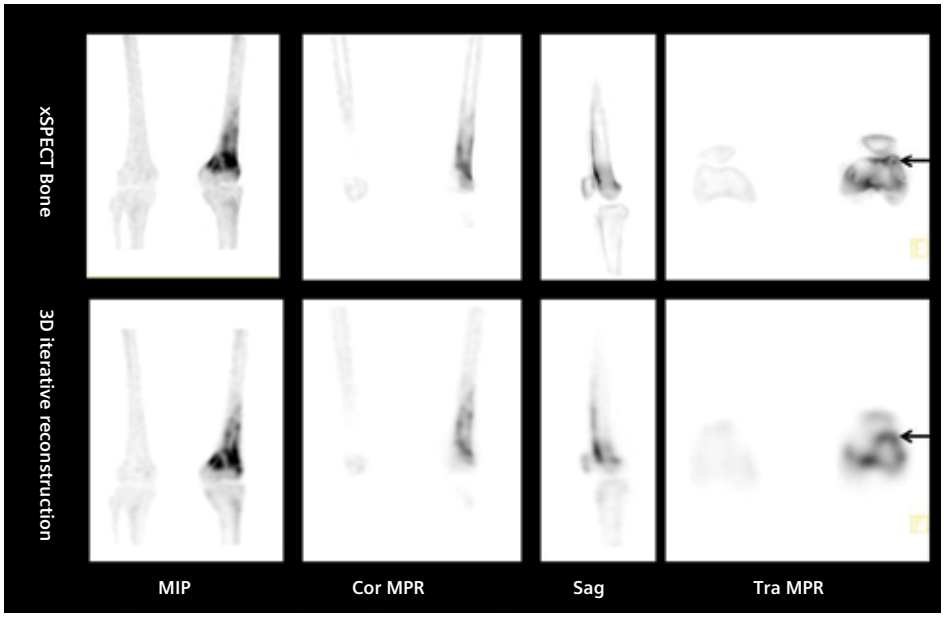

Figure 1: Comparison between 3D iterative reconstruction and xSPECT Bone shows sharp delineation of increased uptake around the cortex of the lower end of the left femur's shaft and extending into the femoral condyles. A small focal uptake in the anterolateral part of the left condyle (*arrows*), clearly delineated on xSPECT Bone, but not clearly discernible on 3D iterative reconstruction, reflects the uptake within the fracture fragment. The central hypodense area in the lower part of the shaft and upper condylar region is sharply delineated on xSPECT Bone.

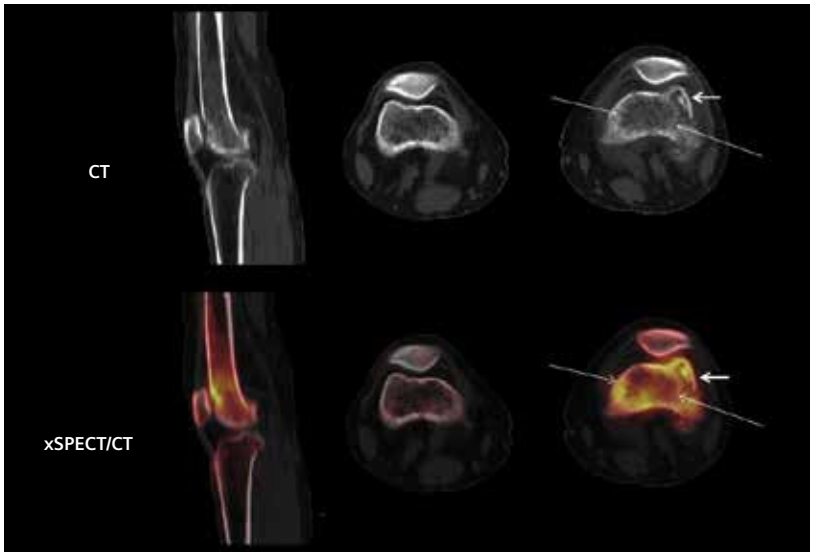

Figure 2: CT and SPECT/CT show an ill-circumscribed mass in the lower end of the left femoral shaft, with minor sclerosis and cortical erosion around it (*thin arrows*), and increased osteoblastic activity shown around the mass corresponding to the zone of cortical erosion (*thin arrows*). There is also an undisplaced fracture in the anterolateral edge of the lateral condyle (*thick arrow*), with well-defined fracture lines seen on CT and a small fracture fragment just below the fractured cortical rim. Fusion of xSPECT and CT shows sharp delineation of the increased uptake in the cortical bone involving the undisplaced fracture, which involves the lateral patellar facet, but does not extend into the knee or lateral patella-femoral joint space. The smaller fracture fragment just below the cortical rim also shows high uptake on xSPECT Bone, reflecting the increased bone turnover in that segment.

Diagnosis

The xSPECT Bone study showed an ill-circumscribed soft tissue mass in the lower end of the left femoral shaft, extending into the condylar region with erosion of spongy and cortical bone around the mass, which suggested a metastatic process (*Figures 1 & 2*). Although breast carcinoma is associated with lytic bone metastases, the CT appearance within the mass was similar to that of normal spongy bone in the opposite femur, and xSPECT Bone shows relative hypointensity compared to the increased osteoblastic activity in the region of cortical erosion. Those features suggested early metastases without a well-defined lytic process. There was also an undisplaced fracture of the anterolateral part of the lower end of the femoral shaft, involving the upper and anterior part of the lateral condyle, which is secondary to the metastatic mass. The fracture involved the lateral patellar facet, but did not extend to the lateral patella-femoral joint space. The posterior patellar surface showed mild increased osteoblastic activity, likely related to disuse of the knee joint and pain and immobilization.

Comments

xSPECT Bone showed sharply delineated uptake in the fracture fragments and involved cortex, and in the margins of erosion around the soft tissue mass, in comparison to the 3D iterative reconstruction images (*Figure 1*). Sharp delineation of the uptake with xSPECT Bone led to more accurate co-registration of increased osteoblastic activity with CT abnormalities like, for example, the small hypermetabolic fracture fragment lying just below the cortical rim. In view of the presence of a malignant erosive lesion in the lower end of the femur that was causing the pathological fracture, the patient was subjected to chemotherapy with subsequent plans of local radiation along with plans of stabilization of the joint in order to allow weight bearing activity.

Conclusion

xSPECT Bone provided sharp delineation and higher contrast, which helped define the fracture fragments secondary to soft tissue metastases in the lower end of the femoral shaft, with improved co-registration and correlation with CT findings, especially of undisplaced fracture fragments. ■

Examination Protocol

Scanner: Symbia Intevo

SPECT	
Injected Dose	20 mCi (740 MBq) ^{99m}Tc MDP
Scan Delay	3 hours
Acquisition	32 stops, 20 sec/stop

CT	
Tube Voltage	130 kV
Tube Current	24 eff mAs
Slice Collimation	16 x 2.5 mm
Slice Thickness	3 mm

* Symbia Intevo and xSPECT Bone are not commercially available in all countries. Due to regulatory reasons their future availability cannot be guaranteed. Please contact your local Siemens organization for further details.

Case 9

Talar Cyst with Insufficiency Fracture Following Ankle Surgery Defined by xSPECT Bone

By Christian Waldherr, MD, and Martin Sonnenschein, MD

Data courtesy of the Department of Radiology & Nuclear Medicine, Klinik Engeried, Bern, Switzerland

History

A 49-year-old male, who had a history of right ankle instability and was treated 8 years back with lateral ankle reconstruction and fixation using a free tendon graft implant through a tunnel drilled laterally through the talus and the fibula, returned to complete weight bearing activity, but with occasional ankle pain. The pain had worsened and weight bearing activity became difficult. The patient underwent an MRI of the right ankle, which suggested a fractured talus cyst. To better evaluate the condition of the ankle bones, the patient underwent a ^{99m}Tc MDP SPECT/CT study.

The study was performed 3 hours following an IV injection of 600 MBq (16.22 mCi) of ^{99m}Tc MDP. The initial planar study was followed by SPECT/CT acquisition. A non-contrast diagnostic CT was performed followed by SPECT acquisition (32 stops per detector, 20 sec/stop). xSPECT Bone* reconstruction was performed using CT-based zone information.

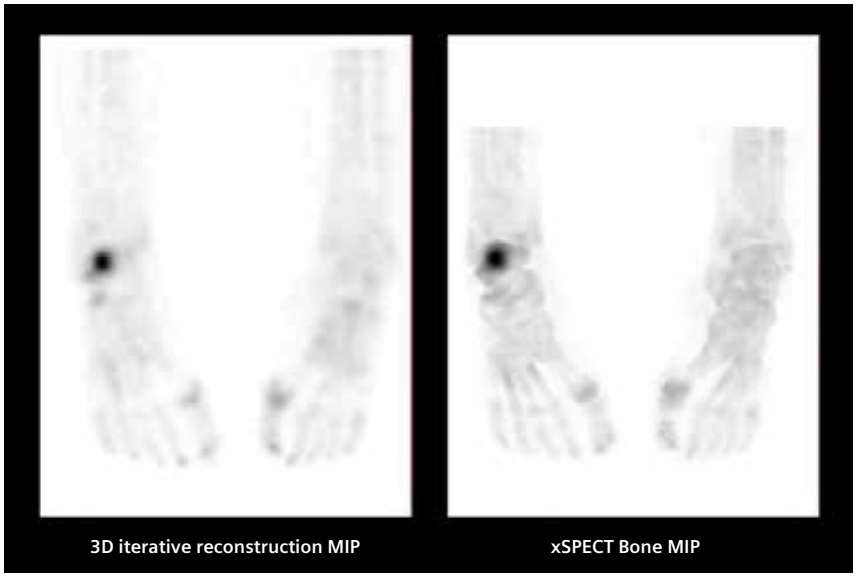

Figure 1: Comparison of maximum intensity projection (MIP) images of standard 3D iterative reconstruction and xSPECT Bone acquisitions of the ankle show focal area of increased uptake in the right talus. The xSPECT Bone images show sharper delineation of the focal increased uptake in the talus and clear visualization of the bony margins of all the tarsal and metatarsal bones, compared to 3D iterative reconstruction. Note the sharp delineation of the talo-tibial joint space even on the MIP image with xSPECT Bone.

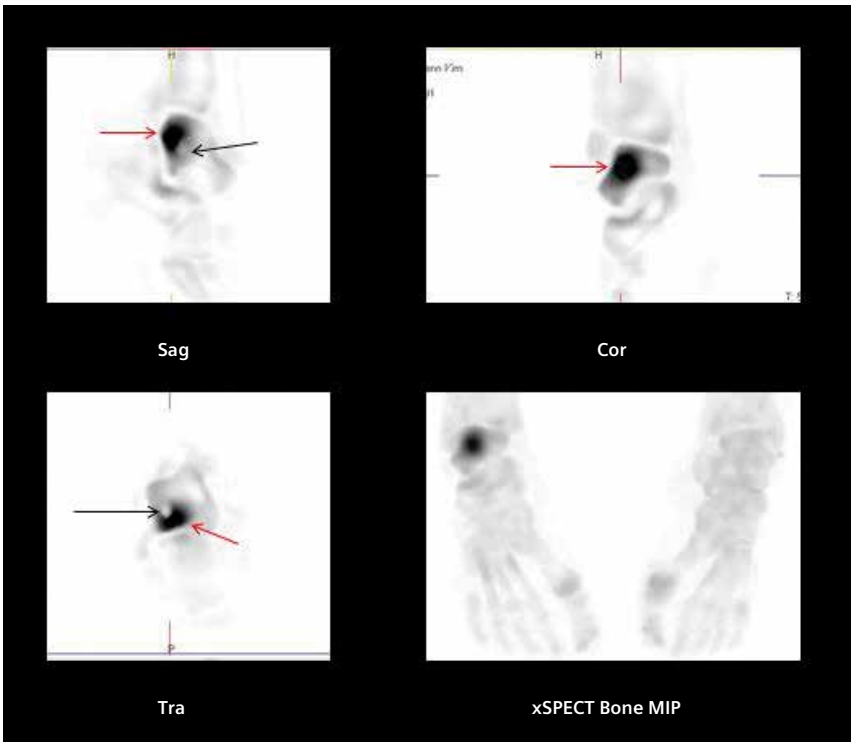

Figure 2: xSPECT Bone multiplanar reconstruction (MPR) images in different orientations show sharp delineation of the focal area of increased uptake within the talus. xSPECT Bone clearly delineates the well-circumscribed hypointense talar cyst (*black arrows*) and sharply defines the focal hypermetabolic area posterior and adjacent to the talar cyst (*red arrows*). The focal area of increased uptake extends onto the adjacent posterior talo-calcaneal articular surface and part of the talo-fibular articular surface, although the joint space appears normal. xSPECT Bone defines the joint space and the cortical margins of the talus and adjacent calcaneal articular surfaces well.

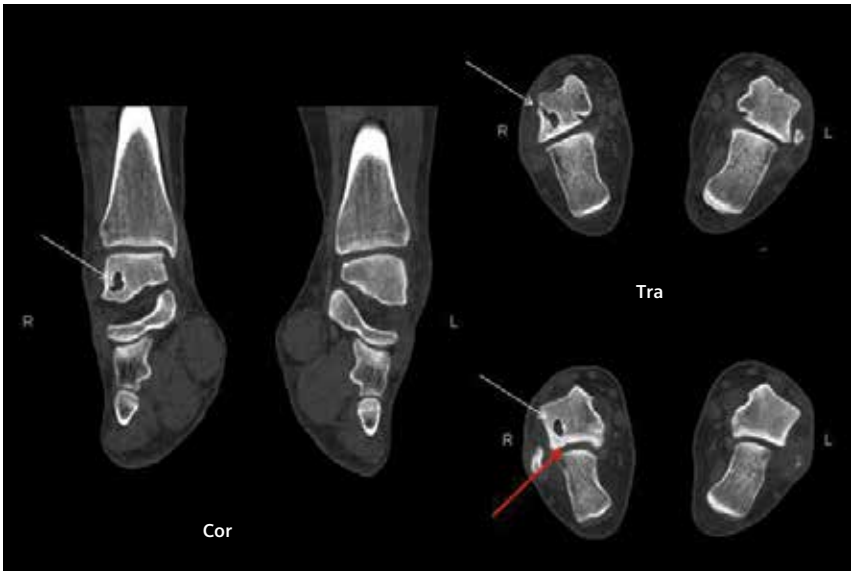

Figure 3: CT images show a cyst in the talus (*white arrows*) arising from the tunnel within the talus drilled during the previous surgery. Transverse CT slices show insufficiency fracture just posterior to the talar cyst (*red arrow*). The talo-calcaneal joint adjacent to the cyst shows slightly increased sclerosis and irregularities in the articular margin, which may be related to arthritic changes following stress on the joint secondary to insufficiency fracture.

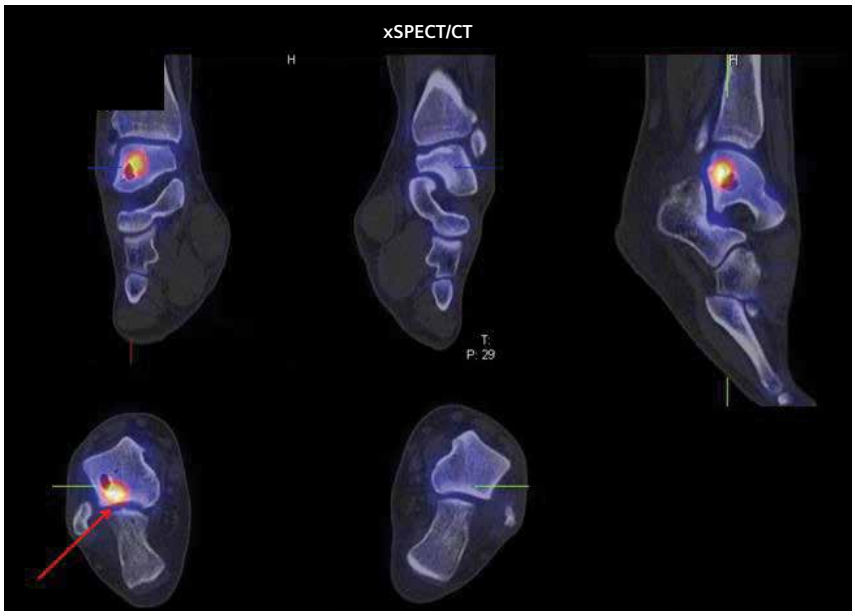

Figure 4: Fusion of CT and xSPECT Bone sharply define the talar cyst arising from the talar tunnel that was created during previous stabilization and tendon fixation surgery, as well as the focal hypermetabolism adjacent to, and posterior to the cyst extending to the adjacent talo-calcaneal articular surface—which also shows irregularity and minor sclerosis (*red arrow*) secondary to reactive arthritic changes following talar insufficiency fracture.

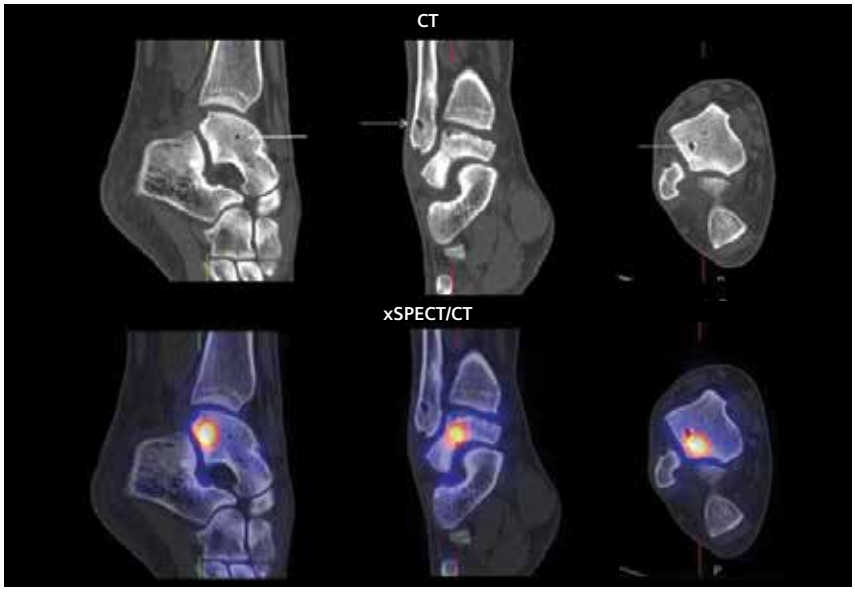

Figure 5: CT and fusion of CT and xSPECT Bone images at slightly different slice and orientation levels show talar tunnel separate from the talar cyst as well as the fibular tunnel drilled as part of the fixation procedure. The focal hypermetabolism can be well localized to a part of the talus posterior to the cyst and adjacent to part of the talo-calcaneal joint.

Diagnosis

CT, xSPECT Bone and fusion images (*Figures 1-5*) clearly defined the talar cyst that had arisen from within the tunnel drilled through the talus during the ankle fixation procedure. The origin of the cyst was most likely due to a foreign body granuloma. The posterior insufficiency fracture in the talus arising from the cyst was well defined on the CT. The bone matrix between cyst and subtalar articular surface was too weak, leading to insufficiency fracture and prolonged healing. The stress on the talo-calcaneal joint adjacent to, and posterior to the cyst following the insufficiency fracture and related instability resulted in focal hypermetabolism delineated on xSPECT Bone, along with slight sclerosis and articular surface irregularity on CT. Due to the size of the cyst, the presence of insufficiency fracture and the adjacent talo-calcaneal joint stress, the decision was made to fill the cyst with bone cement.

Figure 6: T1 MR sagittal image shows hypointensity in the posterior part of the talus involving the talar articular surface of the talo-calcaneal joint, which reflects loss of normal marrow intensity secondary to erosion, edema and arthritic changes in the articular surface.

Comments

xSPECT Bone sharply defined the focal hypermetabolism within the talus. Sharp definition of the lesion and adjacent talar cyst and tunnel, as well as that of the cortical margins of adjacent bones by xSPECT Bone, led to a perfect fusion of xSPECT Bone with CT, thereby enabling the assessment of talo-calcaneal joint stress-related hypermetabolism associated with the insufficiency fracture, which was visualized posteriorly on CT extending to the talar articular surface of the talo-calcaneal joint.

Conclusion

The above clinical case example highlights the sharp lesion definition by xSPECT Bone, which improves co-registration with CT and improves visual clarity of talo-calcaneal joint stress and talar insufficiency fracture. ■

Examination Protocol

Scanner: Symbia Intevo™*

SPECT	
Injected Dose	600 MBq (16.22 mCi) ^{99m}Tc MDP
Scan Delay	3 hours
Acquisition	64 projections, 20 sec/stop

CT	Non-contrast diagnostic
Tube Voltage	110 kV
Tube Current	120 eff mAs
Slice Collimation	16 x 2.5 mm
Slice Thickness	3 mm

* Symbia Intevo and xSPECT Bone are not commercially available in all countries. Due to regulatory reasons their future availability cannot be guaranteed. Please contact your local Siemens organization for further details.

The statements by Siemens customers described herein are based on results that were achieved in the customer's unique setting. Since there is no "typical" hospital and many variables exist (e.g., hospital size, case mix, level of IT adoption) there can be no guarantee that other customers will achieve the same results.

Case 10

Talo-tibial Impingement Secondary to Misplacement of Fixation Screw Characterized with xSPECT Bone

By Christian Waldherr, MD, and Martin Sonnenschein, MD

Data courtesy of the Department of Radiology & Nuclear Medicine, Klinik Engeried, Bern, Switzerland

History

A 52-year-old man with a fracture of the talus secondary to a road accident was treated with internal fixation with multiple screws. Following surgery, the patient complained of left ankle pain during weight bearing activity, as well as sudden severe pain during foot movement, especially during dorsiflexion.

A ^{99m}Tc MDP bone SPECT/CT was performed with xSPECT Bone* reconstruction to evaluate for skeletal pathology. Initial dynamic perfusion and blood pool images were performed immediately following an IV injection of 600 MBq (16.22 mCi) of ^{99m}Tc MDP. A delayed planar study was performed after 3 hours, followed by SPECT/CT acquisition. A non-contrast diagnostic CT was performed, followed by SPECT acquisition (32 stops per detector 20 sec/stop). xSPECT Bone reconstruction was performed using CT-based zone information.

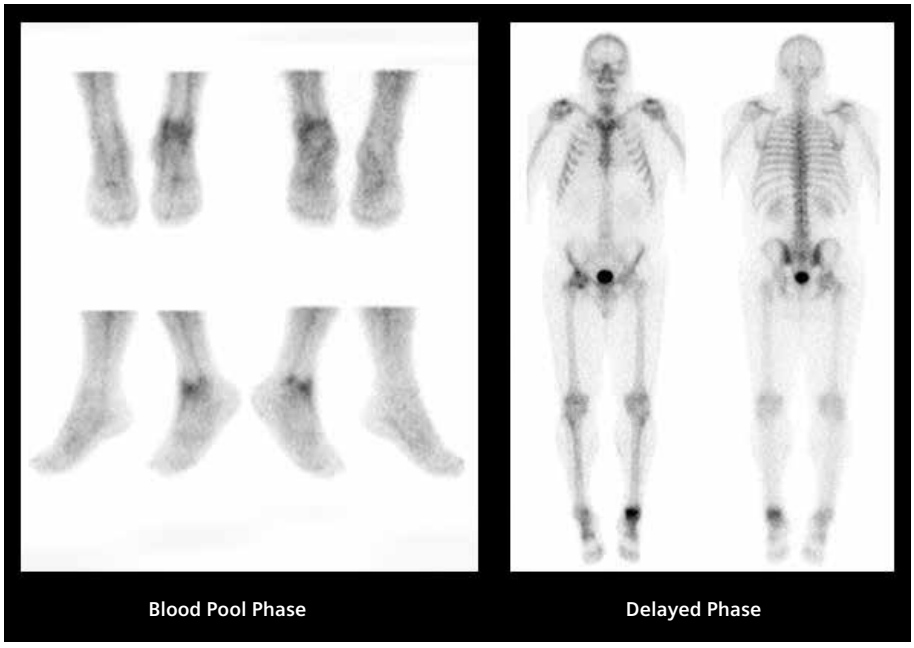

Figure 1: Initial blood pool images show focal hyperemia in the left ankle joint more in the medial aspect. The delayed whole-body planar images show increased uptake in the left ankle joint more on the medial side.

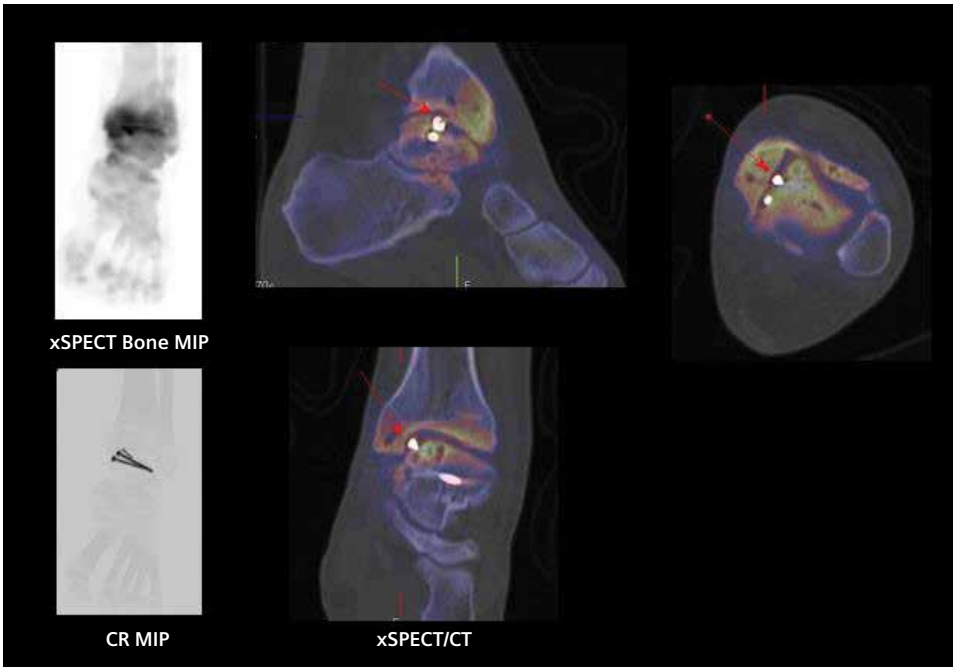

Figure 2: xSPECT Bone maximum intensity projection (MIP) image shows sharp delineation of skeletal hypermetabolism in the talo-tibial joint space, more towards the medial end. The adjacent tibial subchondral bone and medial malleolus also show increased uptake. The CT MIP image shows the lateral orientation of the 3 talar fixation screws, each of which are also delineated in the CT and fused images. xSPECT Bone and CT fused images show skeletal hypermetabolism in the entire articular surface of the lower end of the tibia and the talar articular surface, most prominently in the medial aspect. Metallic hyperdensity within the joint space suggests extrusion of one end of a talar fixation screw into the ankle joint (*arrows*), which is suggested to lead to impingement between the tibial and talar articular surface with resultant osteochondral erosion, osteoarthritis, subchondral multiple small cyst formation and mild sclerosis. There is slight narrowing of joint space and irregularities in the joint surfaces due to impingement. Increased tracer uptake in the articular surface and subchondral space reflects osteoarthritic changes and reactive stress secondary to impingement.

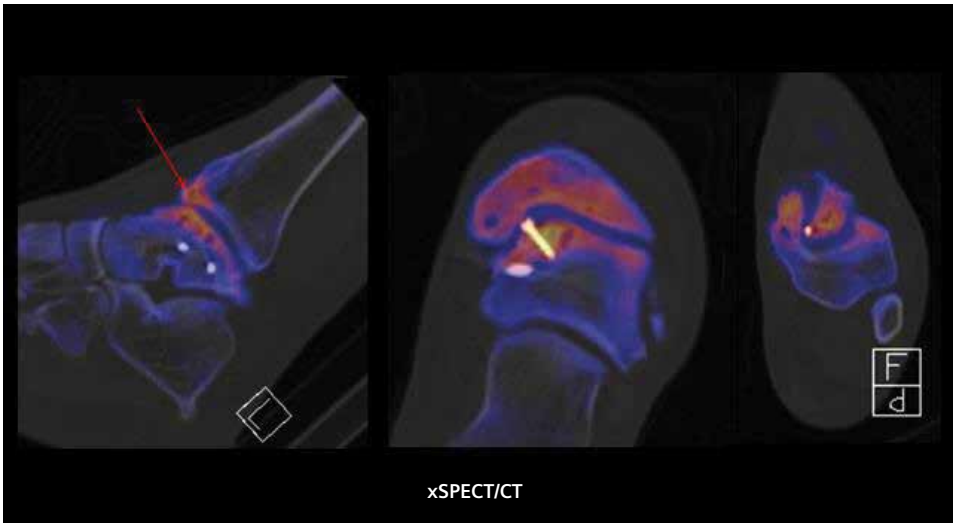

Figure 3: xSPECT Bone and CT fusion images clearly demonstrate the extruded end of the talar fixation screw into the talo-tibial joint space, along with presence of multiple subchondral cysts and skeletal hypermetabolism throughout the articular surface and periarticular bone. Increased uptake in the anterior edge of the tibia (*red arrow*) with corresponding hypermetabolism in the adjacent talar dome suggests anterior impingement of the edge of the lower end of the tibial shaft, with the anterior talar articular surface, which is probably secondary to irregularities and erosion in the surface of the talar articular cartilage, secondary to impingement and fracture-related distortions.

Figure 4: Sagittal and coronal CT reconstructions show extruded end of metallic talar fixation screw (*red arrow*) leading to impingement of the talo-tibial joint with resultant irregularity and erosion of the articular surface. The severity of the osteochondral degeneration is defined by the multiple subchondral cysts both in the talar and tibial periarticular bone (*white arrows*). Some talar subchondral cysts appear very close to the articular surface and almost extruding into the joint space.

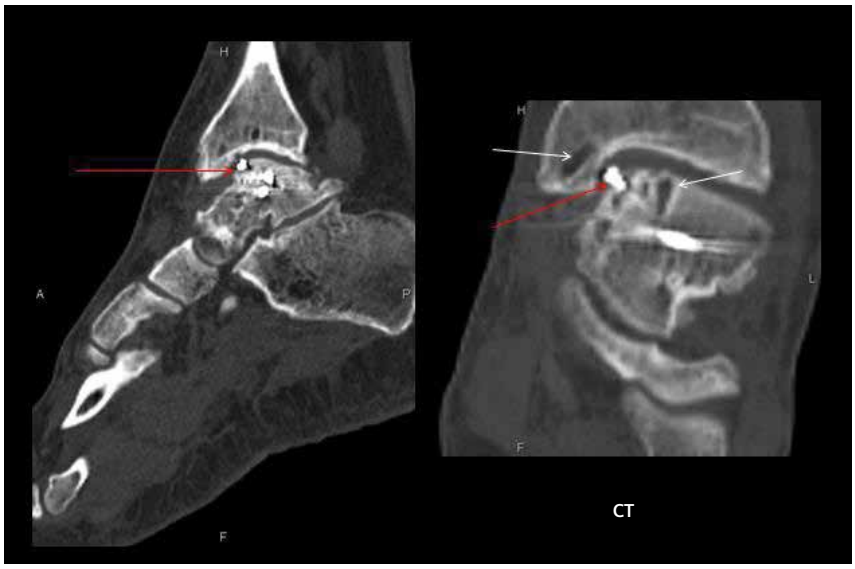

Figure 5: Fused images of CT and xSPECT Bone show increased uptake in the anterior lip of the tibial condyle, which reflects anterior impingement between the anterior edge of the tibial articular surface and the talar articular surface (*red arrow*). The talar articular surface appears irregular with multiple subchondral cysts and skeletal hypermetabolism throughout the articular surface, reflecting osteoarthritic changes. The medial malleolus of the tibia also shows focal increase in uptake (*white arrow*), probably secondary to reactive changes due to impingement in the medial aspect of the talo-tibial joint, due to the extruded end of the second talar screw that is visualized in the coronal images.

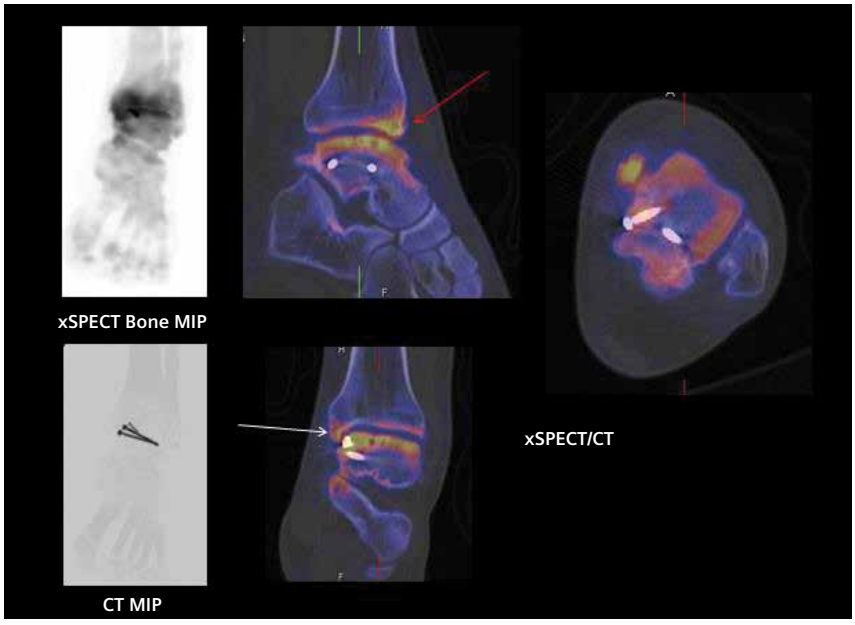

Diagnosis

The CT and fused images in *Figures 2-5* showed extrusion of one end of two talar fixations screws into the talo-tibial joint space, thereby causing impingement of the articular surfaces of the tibia and talus in the central and medial aspect. This may be related to improper positioning of the screws during surgery or extrusion secondary to weakness in the talar bone. The resulting osteoarthritis was associated with articular surface irregularity, significant osteochondral sclerosis and subchondral cyst formation. There was also anterior impingement between the anterior lip of the lower end of the tibia and the adjacent talar dome, which also causes reactive stress and hypermetabolism.

Comments

Diagnostic CT and xSPECT Bone were instrumental in clearly demonstrating the extrusion of the end of two talar fixation screws into the ankle joint space, which led to impingement of the talar and tibial articular surface with resultant severe osteoarthritic changes. xSPECT Bone sharply defined

the linear uptake in the articular surface, within the subchondral bone and in the anterior lip of the lower end of tibia related to the anterior impingement. The articular surfaces and the corresponding osteochondral hypermetabolism were well defined on xSPECT Bone and this helped correlating the uptake with the osteochondral sclerosis, cyst formation and articular surface erosions, due to perfect fusion of the CT and xSPECT Bone without any spillage of activity into the joint space (which is often seen in standard 3D iterative SPECT reconstructions). CT helped define the exact position of the extruding end of the talar screws and suggested impingement of the articular surfaces due to extrusion, rather than other causes like articular surface irregularities. The surface erosion, irregular articular surface, reactive sclerosis and subchondral cyst formation are secondary to the extrusion of the screws.

Conclusion

Sharp delineation of bony hypermetabolism in the tarsal bones due to xSPECT Bone led to perfect co-registration with diagnostic CT, which improved visual clarity of delineation of impingement of talar and tibial articular surfaces secondary to extrusion of talar fixation screws. ■

Examination Protocol

Scanner: Symbia Intevo™*

SPECT	
Injected Dose	600 MBq (16.22 mCi) ^{99m}Tc MDP
Scan Delay	3 hours
Acquisition	64 projections, 20 sec/stop

CT	Non-contrast diagnostic
Tube Voltage	113 kV
Tube Current	36 eff mAs
Slice Collimation	16 x 2.5 mm
Slice Thickness	3 mm

* Symbia Intevo and xSPECT Bone are not commercially available in all countries. Due to regulatory reasons their future availability cannot be guaranteed. Please contact your local Siemens organization for further details.

Case 11

Severe Intervertebral Disc Degeneration with Approximation of Spinous Processes with Inflammation (Baastrup's Sign) Delineated Using xSPECT Bone

By Partha Ghosh, MD, Molecular Imaging Business Unit, Siemens Healthcare

Data courtesy information on file

History

A 67-year-old male, who had a long-standing history of lumbar vertebral disc degeneration that was treated with a laminectomy of the L3-L5 vertebrae, presented with severe pain in the back originating in the upper lumbar vertebrae with aggravation during vertebral extension. In view of the patient's history, he was immediately referred for ^{99m}Tc MDP bone SPECT/CT.

The study was performed 3 hours following an IV injection of 925 MBq (25 mCi) ^{99m}Tc MDP. A non-contrast diagnostic CT was performed, followed by SPECT acquisition (32 stops, 20 sec/stop). xSPECT Bone* reconstructions were performed using CT-based zone maps. xSPECT Bone reconstructions were fused with diagnostic CT for evaluation.

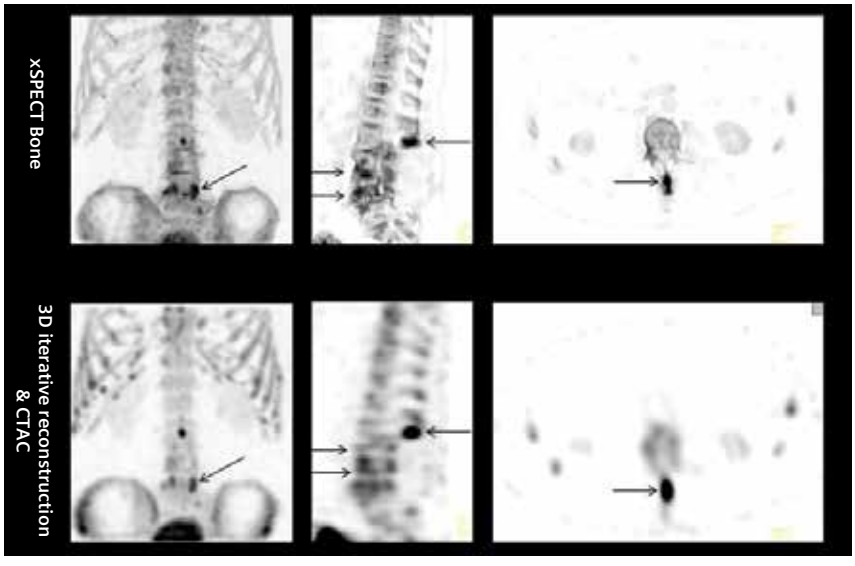

Figure 1: Comparison of 3D iterative reconstruction and xSPECT Bone reconstruction of attenuation-corrected SPECT of the lumbar and lower thoracic spine show severe degenerative changes in the L4-L5 vertebral end plates (*arrows*), with severe decrease in intervertebral disc space. There are also considerable degenerative changes in the L3-L4 disc space (*arrows*). There is a focal area of intense tracer uptake in the spinous process of L2 vertebrae (*arrow*), which also appears to be closely approximated with the spinous process of the L1 vertebrae. Compared to 3D iterative reconstruction, xSPECT Bone shows sharp definition of the end plate hypermetabolism and an accurate representation of two distinct focal uptakes at the end of the L2 spinous process corresponding to two hypertrophied areas. On 3D iterative reconstruction, it appears as a single hot spot.

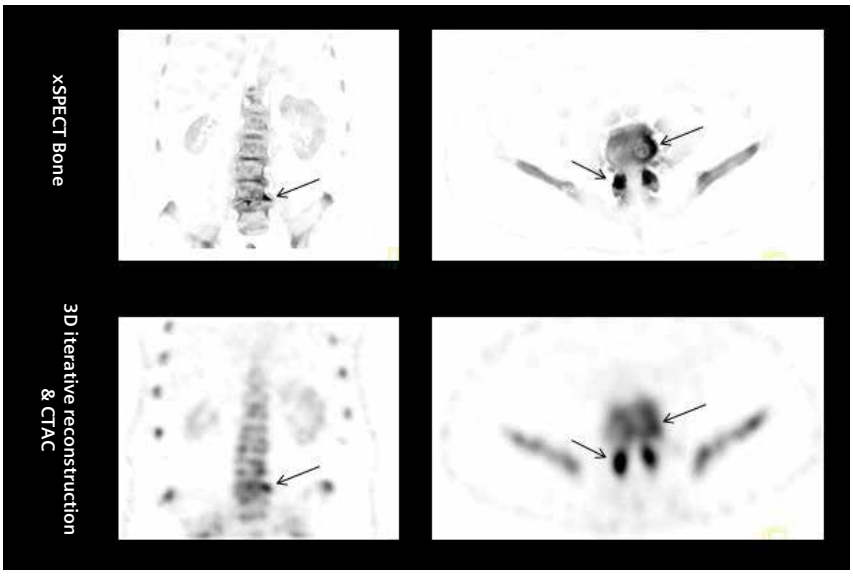

Figure 2: Comparison of 3D iterative reconstruction and xSPECT Bone reconstruction shows severe degenerative changes in the L4-L5 vertebral end plates (*arrows*), along with disc space narrowing. There is also bilateral vertebral facet arthropathy (*arrows*). Compared to 3D iterative reconstruction, xSPECT Bone shows sharper definition of vertebral end plate hypermetabolism and sharply defines outlines of vertebral bodies, pedicles, spinous processes and intervertebral facets. The facet joint arthritic changes are sharply defined on xSPECT Bone, while uptake on 3D iterative reconstruction demonstrates ill-defined margins.

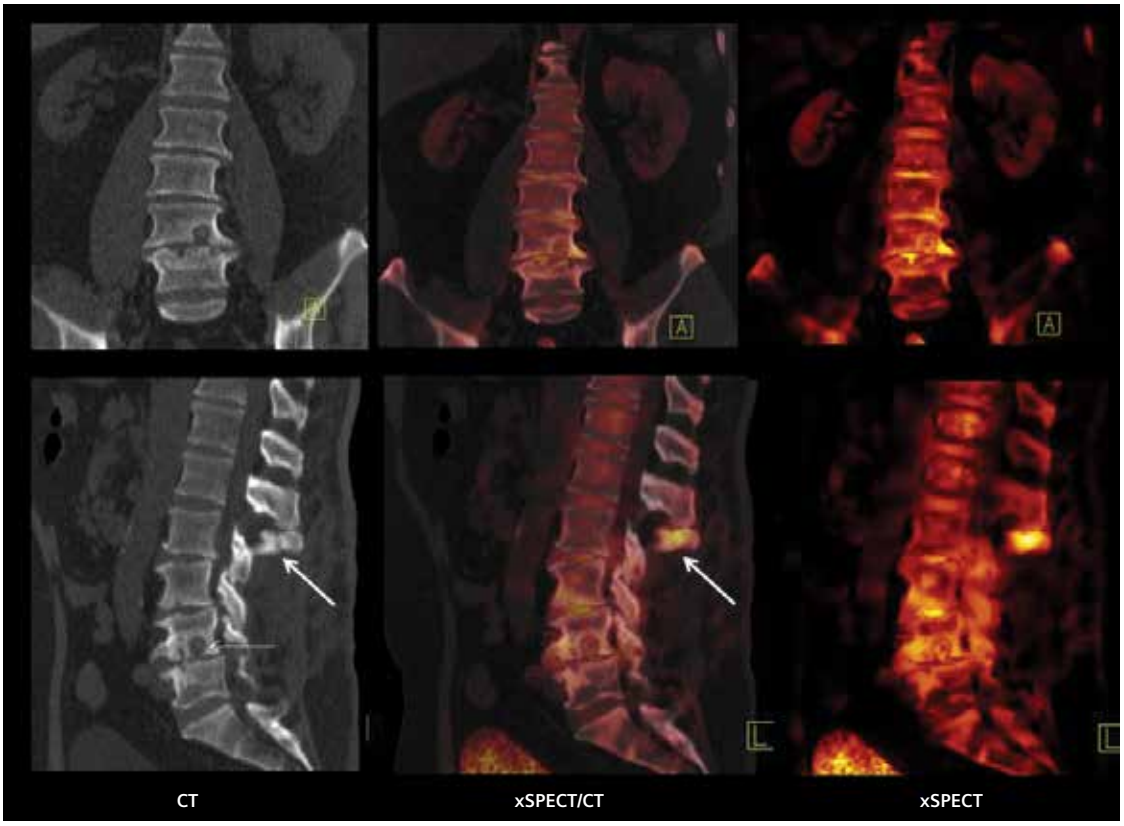

Figure 3: CT, xSPECT Bone and fusion images show severe degenerative changes in L4-L5 vertebral end plates, with associated hypermetabolism in the end plates, adjacent vertebral body and pedicles. The vertebral end plates in L4 and L5 show severe erosion with large subchondral cyst formation (*thin white arrow*), which communicates with the intervertebral disc space along with adjacent reactive sclerosis with resultant hypermetabolism. There is also severe decrease in L4-L5 joint space, with distortion of the normal alignment of lumbar vertebrae. Both L3-L4 and L2-L3 intervertebral disc spaces are slightly decreased along with minor lumbar scoliosis. The spinous process of L2 vertebrae is closely approximating the spinous process of L1 vertebrae with contact secondary to the decrease in normal lumbar lordosis due to narrowing in lumbar intervertebral disc spaces. There is a small fracture line across the L2 spinous process (*bold white arrow*); this corresponds to the site of maximum focal hypermetabolism (*bold white arrow*). The focal hypermetabolism, linear fracture line and associated bony hypertrophy at the end of L2 spinous process is secondary to repeated stress to the end of the spinous process, secondary to contact and friction with the adjacent L1 spinous process (Baastrup's sign).

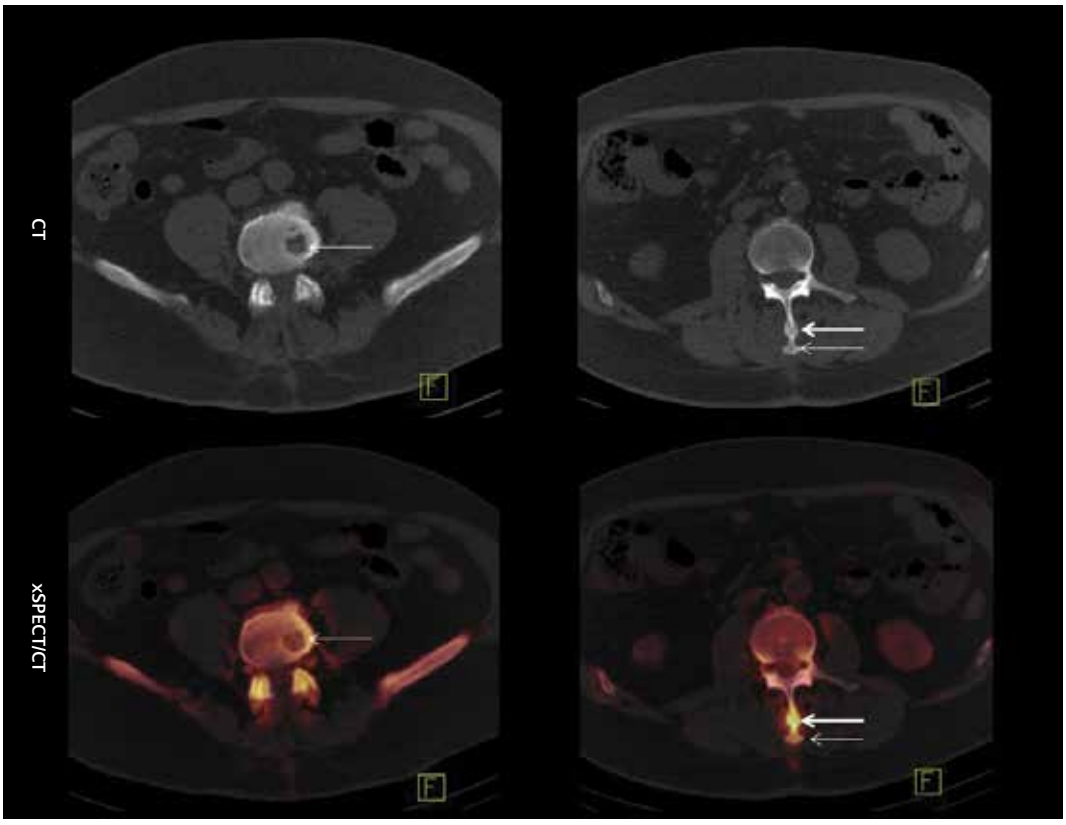

Figure 4: CT and fusion of xSPECT Bone and CT through the L4 end plate (left column), show a large subchondral cyst (*arrows*) in the L4 vertebral end plate, with reactive hypermetabolism in the cyst margin and adjacent part of the end plate, as well as bilateral intervertebral facet arthropathy. Images through the spinous process of the L2 vertebrae (right column) show hypertrophied ends of the spinous process with hypermetabolism (*arrows*) that is secondary to approximation and friction with the adjacent L1 spinous process (Baastrup's sign). The fracture line in the L2 spinous process, the bony hypertrophy as a reaction to the fracture and related friction due to approximation with the spinous process above, and the resultant hypermetabolism in the region of the fracture and hypertrophy is clearly delineated (*bold white arrow*) in the images with fusion of CT and xSPECT Bone.

Diagnosis

As depicted in the CT, xSPECT Bone and fused images (*Figure 1-4*), there was severe degenerative change in the L4-L5 disc space, with severe erosion of the vertebral end plates with subchondral cyst formation, sclerosis, severe disc space narrowing, and characteristic hypermetabolism in the end plate and adjacent subchondral bone. The L3-L4 and L2-L3 disc spaces also showed a lesser degree of degenerative changes and narrowing with characteristic hypermetabolism. Due to asymmetrical decreases in disc space, and misalignment of the lumbar vertebrae due to decrease in normal lordosis, there was abnormal approximation of the L2 spinous process to the adjacent L1 spinous process. The resultant friction and bony stress had resulted in two regions of hypertrophy with corresponding hypermetabolism—one at the very end of the L2 spinous process and another slightly proximally (*Figure 4*), which was the site of the fracture of the spinous process and the site of maximum friction with the L1 spinous process (Baastrup's sign). A fracture line in this region in the L2 spinous process was well delineated on CT, and the bony hypertrophy and hypermetabolism demonstrated on CT and xSPECT Bone reflected the reactive changes secondary to chronic bony stress and related fracture.

Comments

CT and xSPECT Bone clearly defined the severity and extent of the intervertebral disc degeneration. It characterized the abnormal L2 spinous process

uptake related to fracture that was caused by approximation to adjacent L1 spinous process, due to alteration of the normal lumbar spinal curvature following loss of intervertebral disc space and associated minor scoliosis. The hypertrophy of the L2 spinous process secondary to the friction and related hypermetabolism was named Baastrup's sign.

Conclusion
Improved definition of vertebral end plate degeneration and spinous process hypermetabolism with xSPECT Bone along with sharp delineation of end plate sclerosis and subchondral cyst formation improved visual definition of severe disc degeneration. ■

Examination Protocol

Scanner: Symbia Intevo™*

SPECT	
Injected Dose	925 MBq (25 mCi) ^{99m}Tc MDP
Scan Delay	3 hours
Acquisition	32 stops, 20 sec/stop

CT	Non-contrast diagnostic
Tube Voltage	110 kV
Tube Current	108 eff mAs
Slice Collimation	16 x 2.5 mm
Slice Thickness	3 mm

* Symbia Intevo and xSPECT Bone are not commercially available in all countries. Due to regulatory reasons their future availability cannot be guaranteed. Please contact your local Siemens organization for further details.

Case 12

xSPECT Bone: Sharper Visualization of Stress Fracture in Pars Interarticularis Related to Lumbar Spondylolysis

By Jerry Froelich, MD

Data courtesy of University of Minnesota, Minneapolis, MN, USA

History
A 17-year-old girl, who was an avid gymnast, presented with intermittent, lower back pain for 2 years. Initially undergoing MRI, the girl was diagnosed with spondylolysis of the L5 vertebrae and was treated with a Boston bracer for 3 months. The lower back pain was not resolved. Subsequently, the patient presented with new upper lumbar discomfort. As such, she underwent a ^{99m}Tc MDP bone SPECT/CT study, using a Symbia Intevo™* scanner. Three hours following an IV injection of 17 mCi (629 MBq) of ^{99m}Tc MDP, an initial planar bone scan was performed, followed by a SPECT/CT of the abdomen and pelvis. A non-contrast diagnostic CT was performed followed by SPECT acquisition (32 stops, 20 sec/stop). Using CT-based zone information, an xSPECT Bone* reconstruction was performed.

Figure 1: Planar whole-body image shows focal area of mildly increased uptake in the right pedicle of the L5 vertebrae.

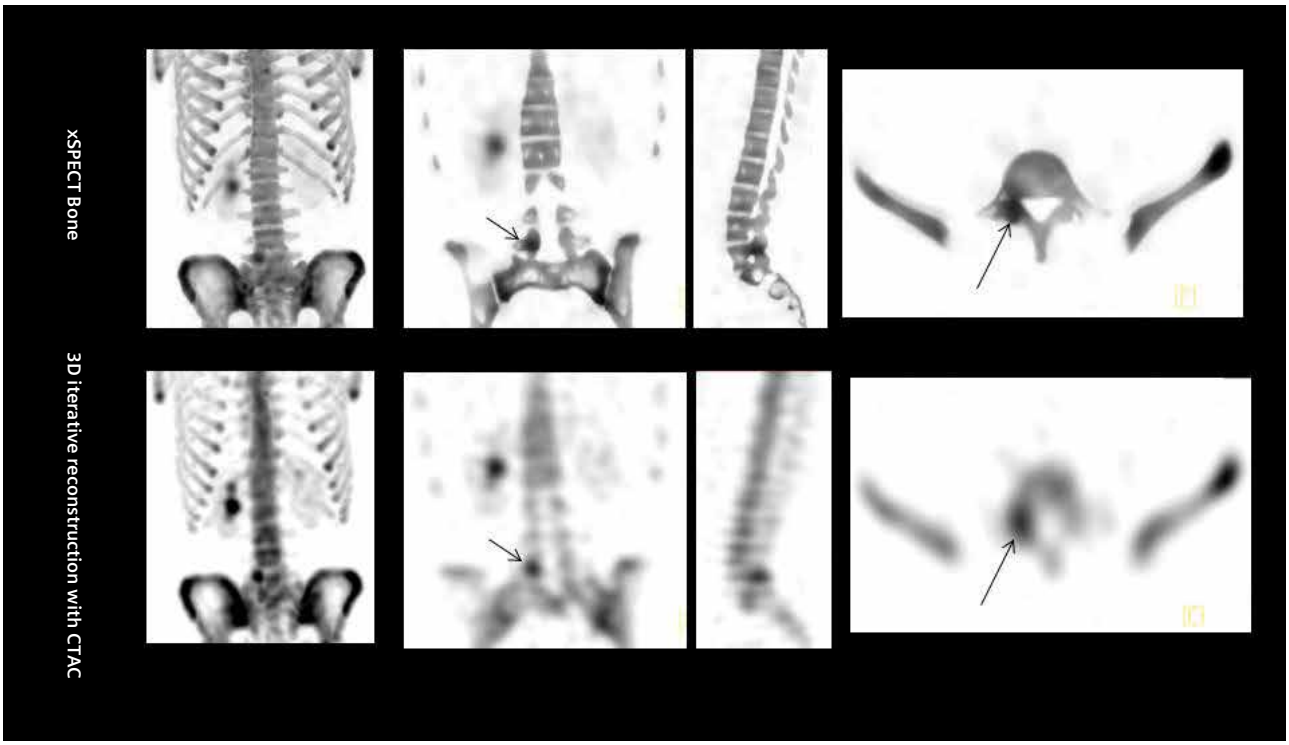

Figure 2: Comparison of 3D iterative reconstruction and xSPECT Bone reconstructions show sharper delineation of the focal area of increased tracer uptake in the right side of the L5 vertebrae, located at the right edge of the lamina. xSPECT Bone sharply delineates the focal hot area and clearly localizes it to the pars interarticularis at the right edge of the right L5 lamina, and in close proximity to the superior articular process.

Diagnosis

CT and xSPECT Bone demonstrated focal skeletal hypermetabolism in the right side pars interarticularis of the L5 vertebrae, which corresponded to a faint transverse lucency and represented a stress fracture in the pars interarticularis with adjacent asymmetric sclerosis (*Figures 2-4*). The pattern was typical of lumbar spondylolysis in young adults, secondary to sports-related repeated lumbar hyperextension with stress reaction and, subsequently, a stress fracture in the pars interarticularis—usually in the L5 or L4, along with reactive sclerosis secondary to bone remodeling. Since the L5 spondylolysis was unilateral in this case, with an absence of any early hypermetabolism in the opposite pars or in the articular facets, the spondylolysis was deemed early without significant instability. Despite the previous attempt to immobilize, immobilization was encouraged to help to promote healing.

Comments

Spondylolysis is defined as a bony defect in the pars interarticularis of the vertebral arch. It presents a weakness or stress fracture in one of the bony bridges that connects the upper with the lower facet joints.

Spondylolysis is a common cause of lower back pain in pre-adolescent and adolescent athletes (50%). For those engaged in activities that appear to place unusual stress on the lower spine, spondylolysis occurs with higher frequency. Gymnasts are particularly vulnerable. A pattern of progression goes from a pars interarticularis stress fracture to unilateral spondylolysis to bilateral spondylolysis. Severe bilateral spondylolysis may progress to spondylolisthesis, which involves sliding forward of one

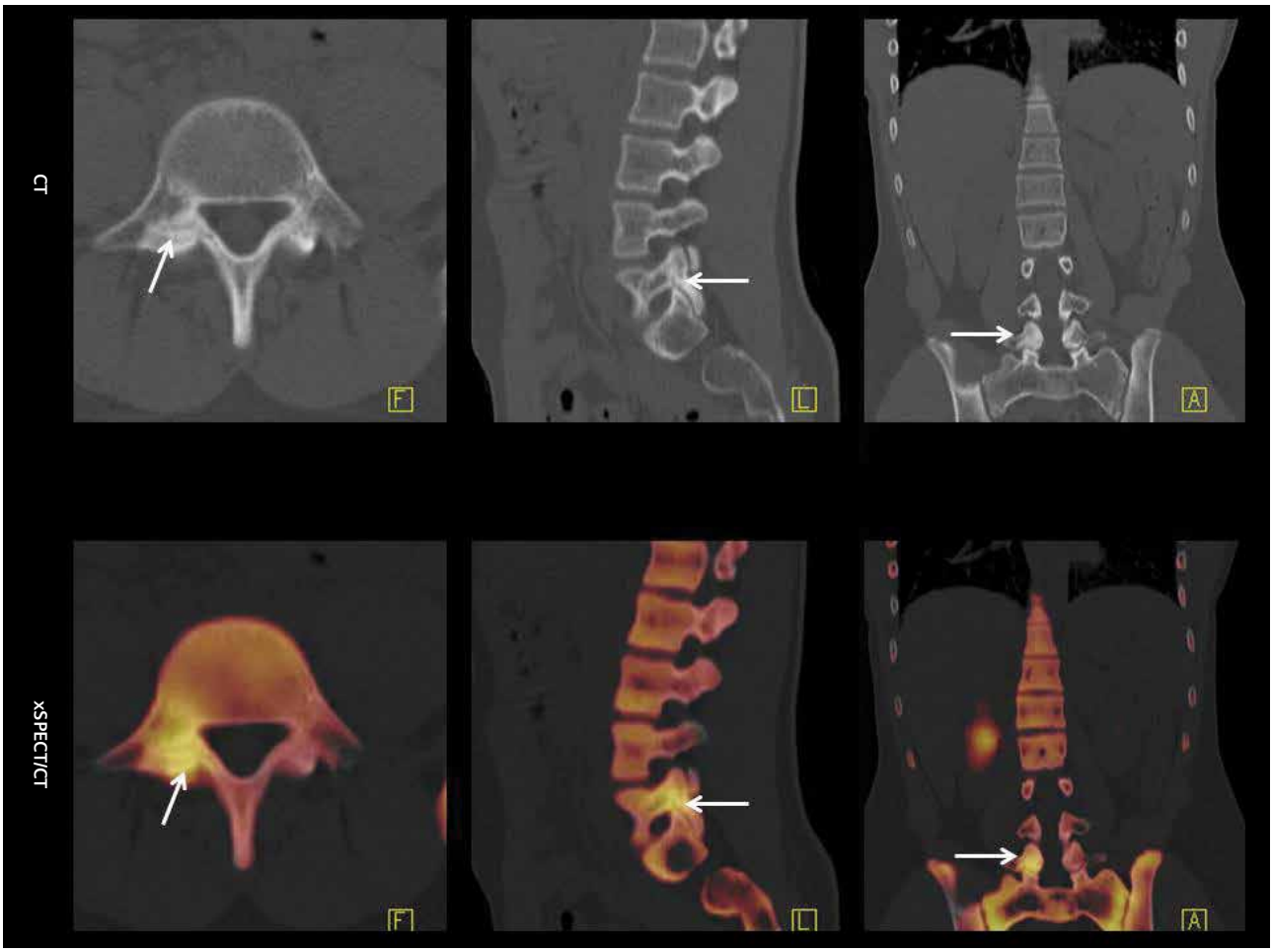

Figure 3: CT shows slightly hypodense transverse fracture line through the pars interarticularis in the right side of the L5 vertebrae (*arrows*) with surrounding reactive sclerosis. Corresponding images with xSPECT Bone and CT fusions show focal skeletal hypermetabolism exactly localized to the transverse fracture line and adjacent sclerosis in the right pars interarticularis, which suggests a stress fracture related to lumbar spondylolysis.

vertebrae over another, and it could compromise the spinal canal.

The vast majority of spondylolitic defects occur at the L5 level (85 - 95%), with L4 being the second most commonly involved level (5-15%). Higher lumbar areas are rarely affected.[1] This type of isthmic spondylolysis results from stress fractures due to mechanical stress in the pars interarticularis, caused by hyperextension and rotation forces. The stress fracture is often visualized as a lucency in the pars interarticularis on CT. Stress reaction of the pars interarticularis is regarded as an early stage of this condition in which no obvious anatomical change is detected. One study performed SPECT with ^{99m}Tc MDP and CT to evaluate 56 pediatric patients with new onset low back pain, related to spondylolysis.[2] A significant portion (19.6%, 11 of 56) of the stress injuries in the pars interarticularis were CT-negative, but were positive stress reactions on the bone SPECT.

In a larger study involving 213 patients, bone SPECT showed increased uptake in 145 patients, while CT identified only 81 patients. In 42.3% of the cases, spondylolysis was localized at L5. 30% of the spondylolysis cases were bilateral and unilateral lesions and were 3 times more likely to occur on the left side.[3]

Conclusion

In the present case, CT demonstrated lucency in the right pars interarticularis of the L5 vertebrae, with adjacent reactive sclerosis that reflected bone healing, probably secondary to the immobilization. xSPECT Bone sharply defined the focal increase uptake in the right L5 pars interarticularlis exactly to the CT abnormality, which helped confirm the diagnosis. ■

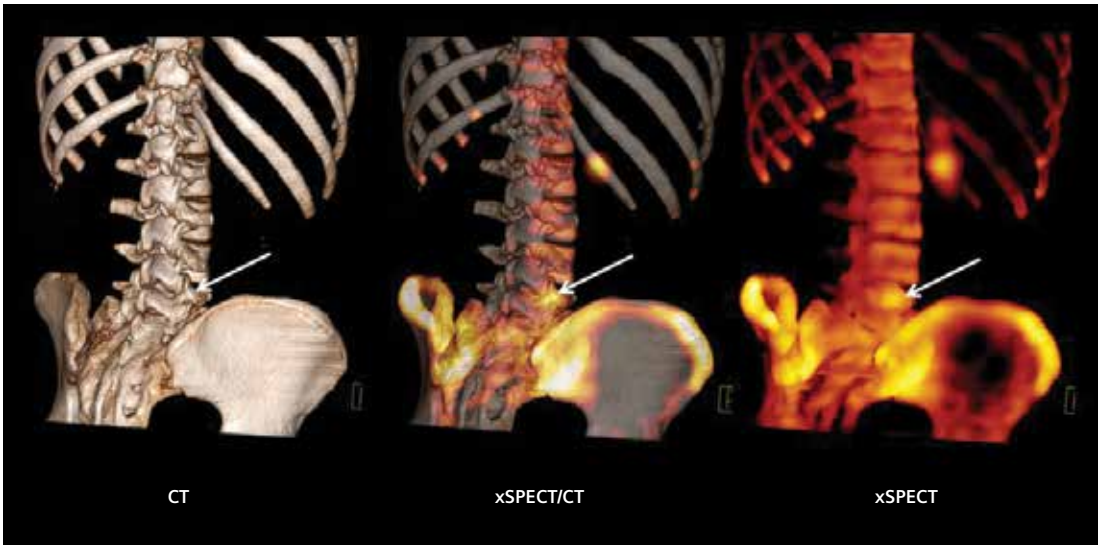

Figure 4: Volume rendering shows the exact location of the stress reaction in right L5 pars interarticularis (*arrows*) with xSPECT Bone and CT fusion.

Examination Protocol

Scanner: Symbia Intevo

SPECT	
Injected Dose	629 MBq (17 mCi) ^{99m}Tc MDP
Scan Delay	3 hours
Acquisition	32 stops, 20 sec/stop

CT	Non-contrast diagnostic
Tube Voltage	130 kV
Tube Current	52 eff mAs
Slice Collimation	6 x 2.0 mm
Slice Thickness	2.5 mm

References:
[1] Standaert et al. *Br J Sports Med*. 2000; 34: 415-422.
[2] Yang et al. *Clin Nucl Med*. 2013 Feb; 38(2): 110-114.
[3] Gregory et al. *Clin J Sport Med*. 2005 Mar; 15(2): 79-86.

* Symbia Intevo and xSPECT Bone are not commercially available in all countries. Due to regulatory reasons their future availability cannot be guaranteed. Please contact your local Siemens organization for further details.

Siemens Healthcare Customer Magazines

Our customer magazine family offers the latest information and background for every healthcare field. From the hospital director to the radiological assistant—here, you can quickly find information relevant to your needs.

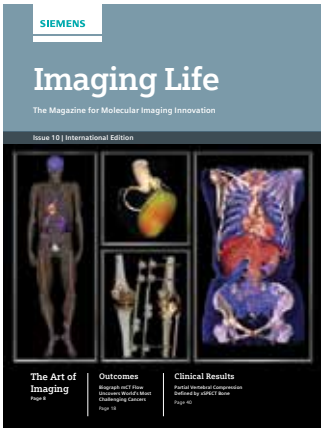

Imaging Life
Everything from the world of molecular imaging innovations.

AXIOM Innovations
Everything from the world of interventional radiology, cardiology, and surgery.

Medical Solutions
Innovations and trends in healthcare. The magazine is designed especially for members of hospital management, administration personnel and heads of medical departments.

Scan and Subscribe!

For current and past issues and to order the magazines, please visit **siemens.com/healthcare-magazine**

MAGNETOM Flash
Everything from the world of magnetic resonance imaging.

SOMATOM Sessions
Everything from the world of computed tomography.

Imaging Life magazines and articles are available for download online at: **siemens.com/imaginglife**

Publisher:
Siemens Medical Solutions USA, Inc.
Molecular Imaging
2501 North Barrington Road
Hoffman Estates, IL 60192
USA
Phone: +1 847 304-7700
siemens.com/mi

Editor: Rhett Morici
rhett.morici@siemens.com

Responsible for Content:
Partha Ghosh, MD
partha.ghosh@siemens.com

Design Consulting:
Clint Poy Design, Georgia, USA

Printer: Tewell Warren Printing,
Colorado, USA

Note in accordance with § 33 Para.1 of the German Federal Data Protection Law: Dispatch is made using an address file which is maintained with the aid of an automated data processing system.

Siemens Molecular Imaging reserves the right to modify the design and specifications contained herein without prior notice. Trademarks and service marks used in this material are property and service names may be trademarks or registered trademarks of their respective holders.

We remind our readers that when printed, X-ray films never disclose all the information content of the original. Artifacts in CT, MR, SPECT, SPECT/CT, PET, PET/CT and PET/MR images are recognizable by their typical features and are generally distinguishable from existing pathology. As referenced below, healthcare practioners are expected to utilize their own learning, training and expertise in evaluating images.

Please contact your local Siemens sales representative for the most current information.

Note: Original images always lose a certain amount of detail when reproduced. All comparative claims derived from competitive data at the time of printing. Data on file.

The consent of the authors and publisher are required for the reprint or reuse of an article. Please contact Siemens for further information. Suggestions, proposals and information are always welcome; they are carefully examined and submitted to the editorial board for attention. Imaging Life is not responsible for loss, damage or any other injury to unsolicited manuscripts or materials.

We welcome your questions and comments about the editorial content of Imaging Life. Please contact us at imaginglife.healthcare@siemens.com.

Imaging Life is available on the internet: siemens.com/imaginglife

Some of the imaging biomarkers in this publication are not currently recognized by the U.S. Food and Drug Administration (FDA) or other regulatory agencies as being safe and effective, and Siemens does not make any claims regarding their use.

Cover Images - University of Minnesota, Minneapolis, MN, USA; Department of Nuclear Medicine, Bundeswehrkrankenhaus Ulm, Ulm, Germany

DISCLAIMERS: Imaging Life: "The information presented in this magazine is for illustration only and is not intended to be relied upon by the reader for instruction as to the practice of medicine. Healthcare practitioners reading this information are reminded that they must use their own learning, training and expertise in dealing with their individual patients. This material does not substitute for that duty and is not intended by Siemens Healthcare to be used for any purpose in that regard." Contrast Agents: "The drugs and doses mentioned herein are consistent with the approved labeling for uses and/or indications of the drug. The treating physician bears the sole responsibility for the diagnosis and treatment of patients, including drugs and doses prescribed in connection with such use. The Operating Instructions must always be strictly followed when operating your Siemens system. The source for the technical data is the corresponding data sheets." Trademarks: "All trademarks mentioned in this document are property of their respective owners." Results: "The outcomes achieved by the Siemens customers described herein were achieved in the customer's unique setting. Since there is no "typical" hospital and many variables exist (e.g., hospital size, case mix, level of IT adoption), there can be no guarantee that others will achieve the same results."

On account of certain regional limitations of sales rights and service availability, we cannot guarantee that all products included in this brochure are available through the Siemens sales organization worldwide. Availability and packaging may vary by country and is subject to change without prior notice. Some/All of the features and products described herein may not be available in the United States.

The information in this document contains general technical descriptions of specifications and options as well as standard and optional features which do not always have to be present in individual cases.

Siemens reserves the right to modify the design, packaging, specifications and options described herein without prior notice.

Please contact your local Siemens sales representative for the most current information.

Note: Any technical data contained in this document may vary within defined tolerances. Original images always lose a certain amount of detail when reproduced.

Global Business Unit
Siemens Medical Solutions USA, Inc.
Molecular Imaging
2501 North Barrington Road
Hoffman Estates, IL 60192
USA
Phone: +1 847 304-7700
siemens.com/mi

Siemens Healthcare Headquarters
Siemens Healthcare GmbH
Henkestraße 127
91052 Erlangen
Germany
Phone: +49 9131 84-0
siemens.com/healthcare

Order No. A91MI-10434-1T-7600 | Printed in USA | MI-2663.RM.CP.TW.1M

siemens.com/imaginglife